

Report No. 3

The Hamburg Sea-Ice Model

Achim Stössel

Max-Planck-Institut für Meteorologie,
Bundesstraße 55, D-2000 Hamburg 13

and

W. Brechner Owens

Woods Hole Oceanographic Institution,
Woods Hole, MA 02543, USA

Edited by: Modellberatungsgruppe
Hamburg, October 1992

Revision 1

Contents

1. SUMMARY PAGE	1
2. MODEL DESCRIPTION	3
2.1. MODEL PHYSICS AND DYNAMICS	3
2.1.1 Sea-ice [SI] model	3
2.1.2 Oceanic mixed-layer [OML] model	9
2.1.3 Atmospheric surface-layer [ASL] parameterization	13
2.1.4 Atmospheric boundary-layer [ABL] model	15
2.2. FINITE DIFFERENCE FORM	17
2.2.1 Momentum equations	19
2.2.2 Continuity equations	21
2.3. MODEL DEVELOPMENT	22
3. SYSTEM DESCRIPTION	23
3.1. FLOW DIAGRAM	23
3.2. DESCRIPTION OF IMPORTANT ROUTINES	29
3.2.1 Details of the important routines	29
4. USER'S MANUAL	35
4.1. RUNNING THE MODEL	35
4.1.1 Batchfile to run the model	35
4.1.2 Script for running the model	35
4.1.3 Standard diagnostic output	36
4.2. PREPROCESSING	37
4.2.1 List of input data sets	37
4.2.2 Details of input data sets	37
4.3. POSTPROCESSING	39
4.3.1 List of output data sets	39
4.3.2 Details of output data sets	39
5. REFERENCES	41

Appendix A	MODEL HEADER	45
Appendix B	CRAY BATCHJOB TO RUN THE MODEL	53
Appendix C	EXAMPLE FOR STANDARD DIAGNOSIC OUTPUT (SISTA)	54
Appendix D	LAND-SEA MASKS	59

1. SUMMARY PAGE

Short description:

The general purpose of the model is to simulate sea ice dynamically as well as thermodynamically. Pure sea-ice models are generally highly dependent on the specified atmospheric and oceanic forcing, especially on the winds and the vertical oceanic heat flux. In order to reduce these dependencies, the sea-ice [SI] model was extended to optionally include a prognostic oceanic mixed layer [OML], a diagnostic atmospheric surface layer [ASL] and/or a diagnostic atmospheric boundary layer [ABL], thus shifting the forcing levels further away from the surface (i.e. from the sea ice) and simultaneously providing a modification of the forcing considering boundary-layer adjustments to the instantaneous sea-ice conditions given by the SI model. A further major extension of the model is the (optional) employment of a prognostic snow layer.

The special application characterising the present code was sea-ice simulation in the Southern Ocean, employing a spherical, circumpolar grid with a resolution of 2.5° in latitude and 5° in longitude, extending from 50° S to 80° S and using a daily time step.

Main Authors of the model:

1. W.D. Hibler III, Thayer School of Engineering, Hanover, NH, USA
2. C. Koch, Friedrich-Wilhelms Universität, Bonn, Germany
3. P. Lemke, AWI, Bremerhaven, Germany
4. W.B. Owens, Oceanographic Institution, Woods Hole, MA, USA
5. A. Stössel, MPI, Hamburg, Germany

Experienced Model Users at DKRZ:

M. Lautenschlager, Model User Support Group

2. MODEL DESCRIPTION

2.1. MODEL PHYSICS AND DYNAMICS

2.1.1 Sea-ice [SI] model

Dynamic part of the model

The dynamic part of the model was developed by Hibler (1979) and is characterised by the following equation of motion:

$$\rho_i h_i \frac{d\mathbf{v}_i}{dt} = -\rho_i h_i f \mathbf{k} \times \mathbf{v}_i + \boldsymbol{\tau}_a + \boldsymbol{\tau}_o - \rho_i h_i g \nabla H + \mathbf{F}, \quad (\text{EQ 1})$$

where

- ρ_i : sea-ice density,
- h_i : mean ice thickness within a grid cell,
- \mathbf{v}_i : ice velocity,
- t : time,
- f : Coriolis parameter,
- \mathbf{k} : unit vector normal to the surface,
- $\boldsymbol{\tau}_a$: stress at the interface atmosphere/sea ice,
- $\boldsymbol{\tau}_o$: stress at the interface sea ice/ocean,
- g : gravitational acceleration,
- H : height of dynamic topography,
- \mathbf{F} : force due to internal ice stress.

The surface stresses are calculated by bulk formulae, e.g. $\boldsymbol{\tau}_o$ as:

$$\boldsymbol{\tau}_o = \rho_o C_{do} |\mathbf{v}_{og} - \mathbf{v}_i| [(\mathbf{v}_{og} - \mathbf{v}_i) \cos \phi_o + \mathbf{k} \times (\mathbf{v}_{og} - \mathbf{v}_i) \sin \phi_o], \quad (\text{EQ 2})$$

where

- ρ_o : sea-water density,
- C_{do} : drag coefficient for the interface sea ice/ocean,
- \mathbf{v}_{og} : geostrophic current,
- ϕ_o : deviation angle.

Here, the relative velocity between ice drift and ocean current is used, whereas in the calculation of $\boldsymbol{\tau}_a$ the ice velocity can be neglected. Since usually $|\mathbf{v}_{og}| < |\mathbf{v}_i|$, $\boldsymbol{\tau}_o$ effectively slows down the movement of ice.

The components of \underline{F} are determined from:

$$F_i = \frac{\partial \sigma_{ij}}{\partial x_j}, \quad (\text{EQ 3})$$

(eqs. (5) and (6) in Hibler (1979)), where σ_{ij} represents the two-dimensional stress tensor. This is considered to obey a constitutive law of a non-linear viscous compressible fluid:

$$\sigma_{ij} = 2\eta \dot{\epsilon}_{ij} + (\zeta - \eta) \dot{\epsilon}_{kk} \delta_{ij} - \frac{P \delta_{ij}}{2}, \quad (\text{EQ 3a})$$

with

$$\zeta = \frac{P}{2\Delta}, \quad (\text{EQ 3b})$$

$$\eta = \frac{\zeta}{e^2}, \quad (\text{EQ 3c})$$

$$P = P^* h_i e^{(-C^* (1 - N_i))}, \quad (\text{EQ 3d})$$

and

$$\Delta = [e^{-2} ((\dot{\epsilon}_{11} - \dot{\epsilon}_{22})^2 + 4\dot{\epsilon}_{12}^2) + (\dot{\epsilon}_{11} + \dot{\epsilon}_{22})^2]^{1/2}, \quad (\text{EQ 3e})$$

where

- P : ice strength,
- P^* : empirical ice strength parameter,
- C^* : empirical constant,
- ζ : bulk viscosity,
- η : shear viscosity,
- e : ratio of compressive to shear strength,
- $\dot{\epsilon}_{ij}$: deformation-rate tensor,
- N_i : ice compactness (= ice coverage per grid cell = ice concentration).

The stress-strain rate relation is described by the associated flow rule (Hibler, 1977). The viscous-plastic rheology represents an elliptical yield curve in principle component stress space, which determines the ratio of compressive to shear strength (Leppäranta and Hibler, 1985).

Continuity equations

The link between the dynamic and the thermodynamic part of the model is given by continuity equations for ice thickness, ice compactness and snow thickness:

$$\frac{\partial h_i}{\partial t} = -\nabla \cdot (v_i h_i) + \left(\frac{\partial h_i}{\partial t}\right)_{th} + diffusion , \quad (\text{EQ 4})$$

$$\frac{\partial N_i}{\partial t} = -\nabla \cdot (v_i N_i) + \left(\frac{\partial N_i}{\partial t}\right)_{op} + \left(\frac{\partial N_i}{\partial t}\right)_{th} + diffusion , \quad (\text{EQ 5})$$

$$\frac{\partial h_{sn}}{\partial t} = -\nabla \cdot (v_i h_{sn}) + \left(\frac{\partial h_{sn}}{\partial t}\right)_{th} + diffusion , \quad (\text{EQ 6})$$

where h_{sn} is the mean snow thickness and where the index th represents thermodynamic terms, which will be illustrated in the next section. The ice velocities in the advection terms are derived from the dynamic part. The term $(\partial N_i / \partial t)_{op}$ in (EQ 5) was introduced according to Hibler (1984) and accounts for the formation of extra open water due to shear deformation. This modification is based on the concept that ridging and creation of open water may occur simultaneously during situations of high ice compactness. That part of the local change of ice compactness yields:

$$\left(\frac{\partial N_i}{\partial t}\right)_{op} = \frac{(1 - P_{op})}{2} \{ \Delta - \dot{\epsilon}_{11} - \dot{\epsilon}_{22} \} , \quad (\text{EQ 7})$$

with

$$P_{op} = \frac{(1 - N_i) [0.5 (1 + N_i) - 0.85]}{0.15 [0.5 \cdot 1.85 - 0.85]} ,$$

which is energetically consistent with the elliptical yield curve mentioned in the previous section. The diffusion terms were introduced for numerical purposes.

Thermodynamic part of the model

In the thermodynamic part of the model the heat balance equation is solved separately for the open water and the ice covered part of a grid cell, following Semtner (1976) and Parkinson and Washington (1979).

Over ice:

$$(1 - \alpha) Q_{sw} + Q_{lw} - \varepsilon \sigma T_s^4 + Q_{se} + Q_{la} + Q_c \equiv Q_a + Q_c = 0 \quad , \quad (\text{EQ 8})$$

where

- α : albedo (of ice or snow),
- Q_{sw} : shortwave radiation heat flux,
- Q_{lw} : longwave radiation heat flux,
- ε : emissivity (of ice or snow),
- σ : Stefan-Boltzmann constant,
- T_s : surface temperature (of ice or snow),
- Q_{se} : sensible heat flux,
- Q_{la} : latent heat flux,
- Q_c : conductive heat flux through the ice,
- Q_a : atmospheric heat flux.

The radiation and turbulent heat fluxes are calculated by standard (bulk) formulae (similar to Parkinson and Washington, 1979). The albedo is allowed to vary with snow cover and freezing or melting conditions.

The conductive heat flux yields:

$$Q_c = \frac{(T_b - T_s) \cdot k_i}{\tilde{h}_i} \quad (\text{EQ 9})$$

where

- T_b : temperature at the ice bottom (= freezing point),
- k_i : thermal conductivity of ice,

and

$$\tilde{h}_i = \frac{\hat{h}_i}{N_i} \quad (\text{EQ 10})$$

where

- \tilde{h}_i : "effective" ice thickness,

with

$$\hat{h}_i = h_i + h_{sn} \frac{k_i}{k_{sn}} \quad (\text{EQ 11})$$

where

- \hat{h}_i : "total" ice thickness,

k_{sn} : thermal conductivity of snow.

For the ice covered part, the heat balance equation (EQ 8) can now be calculated with the locally existing effective ice thickness (EQ 10). Changing the actual snow thickness into an equivalent ice thickness, the total ice thickness (EQ 11) implicitly includes the insulation effect of snow.

T_s is determined from (EQ 8) by iteration. If T_s is $> 0^\circ\text{C}$, it is set to 0°C and (EQ 8) identical to $-\rho_i L_f (\partial \tilde{h}_i / \partial t)_s$ in order to derive the change of ice thickness due to surface melt (Maykut, 1982):

$$\left(\frac{\partial \tilde{h}_i}{\partial t}\right)_s = \frac{1}{\rho_i L_f} (-Q_a - Q_c) \quad , \quad (\text{EQ 12})$$

where L_f : latent heat of fusion.

At the bottom of the ice:

$$\left(\frac{\partial \tilde{h}_i}{\partial t}\right)_b = \frac{1}{\rho_i L_f} (Q_c - Q_o) \quad , \quad (\text{EQ 13})$$

where Q_o : oceanic heat flux.

Thus the total change of the effective ice thickness yields:

$$\left(\frac{\partial \tilde{h}_i}{\partial t}\right) = \left(\frac{\partial \tilde{h}_i}{\partial t}\right)_b + \left(\frac{\partial \tilde{h}_i}{\partial t}\right)_s \delta_{jk} \quad , \quad (\text{EQ 14})$$

where $j = k$, if $T_s = 0^\circ\text{C}$,

and $\delta_{jk} = \begin{cases} 1, & \text{if } j = k \\ 0, & \text{if } j \neq k \end{cases}$.

In order to include the new-ice production in the ice free part of a grid cell, the total thermodynamic change of ice thickness (Hibler, 1979; Owens and Lemke, 1990) combines to:

$$\left(\frac{\partial h_i}{\partial t}\right)_{th} = N_i \left(\frac{\partial \tilde{h}_i}{\partial t}\right) \delta_{jk} + (1 - N_i) \left(\frac{\partial h'_i}{\partial t}\right) \quad , \quad (\text{EQ 15})$$

where $j \neq k$, if $(\partial \tilde{h}_i / \partial t) < 0$ and $h_{sn} > 0$,

h'_i : new-ice thickness.

Here, $\delta_{jk} = 0$ applies for snow, which in this case is melted first according to (EQ 17). The new-ice production, given in the second term of (EQ 15), is determined from (EQ 8), using the albedo of water and the ocean surface temperature (i.e. the mixed-layer temperature).

The thermodynamic change of ice compactness is determined empirically (Hibler, 1979):

$$\left(\frac{\partial N_i}{\partial t}\right)_{th} = \frac{(1 - N_i)}{h^*} \left(\frac{\partial h'_i}{\partial t}\right) \delta_{jk} + \frac{N_i}{2h_i} \left(\frac{\partial h_i}{\partial t}\right)_{th} \delta_{ln} , \quad (\text{EQ 16})$$

where $j = k$, if $(\partial h'_i / \partial t) > 0$,
 $l = n$, if $(\partial h_i / \partial t)_{th} < 0$,
 h^* : empirical parameter.

In the first term on the right hand side of (EQ 16) h^* determines the rate of lead closing. In the second term it is assumed that in the case of ice melt, the ice within a grid cell is equally distributed between twice the mean ice thickness and zero. That part of the grid cell, which became ice free due to vertical ice melt, subsequently determines the reduction of ice compactness, i.e. the so called lateral ice melt.

According to Owens and Lemke (1990) the thermodynamic change of snow thickness is treated as follows:

$$\left(\frac{\partial h_{sn}}{\partial t}\right)_{th} = N_i P_w \frac{\rho_w}{\rho_{sn}} \delta_{jk} + N_i \left(\frac{\partial \tilde{h}_i}{\partial t}\right) \frac{\rho_i}{\rho_{sn}} \delta_{ln} , \quad (\text{EQ 17})$$

where $j = k$, if $T_a \leq 0^\circ C$,
 $l = n$, if $(\partial \tilde{h}_i / \partial t) < 0$ and $h_{sn} > 0$,
 P_w : precipitation rate,
 ρ_w : fresh-water density,
 ρ_{sn} : snow density.

In order to avoid exaggerated accumulation of snow on multi-year ice, a snow to ice conversion according to Stössel and Claussen (1992) is introduced. It applies whenever the weight of the snow exceeds the buoyancy of the ice-plus-snow column to an extent that the snow submerges below the water line.

A further modification to Hibler (1979) is a seven-level ice-thickness parameterization according to Hibler (1984):

$$\left(\frac{\partial \tilde{h}_i}{\partial t}\right) \equiv w_i(\tilde{h}_i) = \frac{1}{n} \sum_{k=1}^n w_i \left(\frac{(2k-1) \tilde{h}_i}{n} \right) , \quad (\text{EQ 18})$$

where $n = 7$: number of levels,
 w_i : ice-growth rate.

With (EQ 18) the heat balance equation is calculated for seven ice-thickness categories, thus taking into account the highly non-linear relationship between growth rate and ice thickness.

2.1.2 Oceanic mixed-layer [OML] model

Conservation of salt and heat

According to Lemke (1987) the vertical profiles of heat and salt are described as follows:

$$\begin{aligned}
 T_o(z_o) &= T_{o1} & \text{for } (0 > z_o > z_{o1}) &= -h_{o1} \\
 T_o(z_o) &= T_{o2} + (T_{o1} - T_{o2}) e^{-\frac{z_o + h_{o1}}{h_{Tc}}} & \text{for } (z_{o1} > z_o > z_{o2}) &,
 \end{aligned}
 \tag{EQ 19}$$

and

$$\begin{aligned}
 S(z_o) &= S_1 & \text{for } (0 > z_o > z_{o1}) &= -h_{o1} \\
 S(z_o) &= S_2 + (S_1 - S_2) e^{-\frac{z_o + h_{o1}}{h_{Hc}}} & \text{for } (z_{o1} > z_o > z_{o2}) &,
 \end{aligned}
 \tag{EQ 20}$$

where

- $T_o(z_o), S(z_o)$: ocean temperature, salinity as function of depth,
- T_{o1}, S_1 : mixed-layer temperature, salinity
- T_{o2}, S_2 : temperature, salinity at the base of the second oceanic layer,
- h_{o1} : thickness (=depth(| z_{o1} |)) of mixed layer,
- z_{o2} : depth of the base of the second oceanic layer,
- h_{Tc} : thermocline thickness,
- h_{Hc} : halocline thickness.

The change of the heat content within the water column from the surface to z_{o2} is given by:

$$\left(\frac{\partial T_{o1}}{\partial t}\right) (h_{o1} + h_{Tc}) + (T_{o1} - T_{o2}) \left(\frac{\partial h_{o1}}{\partial t} + \frac{\partial h_{Tc}}{\partial t}\right) = \frac{Q_a}{\rho_a c_a} + w^* (T_{o2} - T_{o1}) \quad , \tag{EQ 21}$$

where

- ρ_a : air density (over the surface),
- c_a : specific heat capacity of air,
- w^* : empirical (upwelling) velocity parameter.

w^* is constant and empirically determined in order to compensate the excess of precipitation over evaporation in high latitudes. For the change of salinity, a corresponding relation is valid. In the following, the equations for the salinity will not be mentioned if they are analogous to the temperature part.

The parameterization of the vertical entrainment

The mixed-layer heat content changes due to the vertical divergence of the heat flux:

$$\frac{\partial T_{o1}}{\partial t} = \left(\frac{Q_a}{\rho_a c_a} + \frac{Q_o}{\rho_o c_o} \right) / h_{o1} \equiv (\tilde{Q}_s + \tilde{Q}_e) / h_{o1}, \quad (\text{EQ 22})$$

where c_o : specific heat of sea water.

I.e., the change of mixed-layer temperature is composed of the atmospheric plus the oceanic heat flux.

The oceanic entrainment heat flux is parameterized as follows:

$$\tilde{Q}_e = (\bar{T}_{Tc} - T_{o1}) w_e, \quad (\text{EQ 23})$$

where

$$\bar{T}_{Tc} = \frac{1}{\delta'} \int_{(-h_{o1} - \delta')}^{-h_{o1}} T_o(z_o) dz_o = T_{o2} + (T_{o2} - T_{o1}) \frac{h_{Tc}}{\delta'} (e^{-\delta'/h_{Tc}} - 1)$$

and w_e : entrainment velocity,
 δ' : turbulent length scale.

This is a modification of the parameterization of Kraus and Turner (1967) in the sense that the entrainment heat flux is not directly dependent on T_{o2} , but rather on a mean temperature within the thermocline.

The local change of the mixed-layer depth is given by:

$$\frac{\partial h_{o1}}{\partial t} = w_e - w^* \quad (\text{EQ 24})$$

Eliminating $Q_a / (\rho_a c_a)$ in (EQ 21) and (EQ 22) finally yields:

$$\frac{\partial h_{Tc}}{\partial t} = \frac{h_{Tc} \frac{\partial T_{o1}}{\partial t} + w_e (\bar{T}_{Tc} - T_{o2})}{T_{o2} - T_{o1}}. \quad (\text{EQ 25})$$

Determining the surface heat flux (\tilde{Q}_s), it is assumed that T_{o1} is at the freezing point as long as sea ice is present, i.e. $\partial T_{o1} / \partial t = 0$. Thus from (EQ 22):

$$\tilde{Q}_s = -\tilde{Q}_e. \quad (\text{EQ 26})$$

The surface salt flux (\tilde{S}_s) is assumed to be composed of the freezing or melting rate (determined by the conductive and the oceanic heat flux) and the net fresh-water flux:

$$\tilde{S}_s = (S_1 - S_i) \left(\frac{\partial h_i}{\partial t} \right)_{th} \frac{\rho_i}{\rho_o} - F S_1 \quad , \quad (\text{EQ 27})$$

where S_1 : mixed-layer salinity,
 S_i : sea-ice salinity,
 F : net fresh-water flux,

and where $(\partial h_i / \partial t)_{th}$ is determined by (EQ 15).

Following Owens and Lemke (1990), the fresh-water flux is given by the following relation, where fresh-water storage in form of snow is included:

$$F = P_w (1 - N_i \delta_{jk}) + \frac{\partial \tilde{h}_i}{\partial t} \frac{\rho_i}{\rho_w} N_i \delta_{ln} \quad , \quad (\text{EQ 28})$$

where $j = k$, if $T_{a1} \leq 0^\circ \text{C}$,
 $l = n$, if $(\partial \tilde{h}_i / \partial t) < 0$ and $h_{sn} > 0$.

Energy balance

To close the system of equations it is assumed that the potential energy due to the surface and entrainment heat and salt fluxes (\tilde{Q}_s , \tilde{Q}_e , \tilde{S}_s , \tilde{S}_e) is balanced by the kinetic energy released from wind stress or ice drift, respectively, and in winter additionally by convection. According to Niiler and Kraus (1977):

$$K - \varepsilon' = \frac{h_{o1}}{2} g [\beta' (\tilde{S}_e - \tilde{S}_s) - \alpha' (\tilde{Q}_e - \tilde{Q}_s)] \quad , \quad (\text{EQ 29})$$

where K : kinetic energy,
 ε' : dissipation term,
 α' : expansion coefficient for temperature,
 β' : expansion coefficient for salinity.

Solving (EQ 29) for the entrainment velocity yields:

$$w_e = \frac{\frac{2KD_m}{g} + h_{o1} D_h \left[\beta' \left(\frac{(S_1 - S_i) Q_a}{\rho_o L_f} - F S_1 \right) \right]}{h_{o1} \left[\beta' (\bar{S}_{Hc} - S_1) + \left(\beta' c_o \frac{S_1 - S_i}{\rho_o L_f} - 2\alpha' \right) (\bar{T}_{Tc} - T_{o1}) \right]} \quad , \quad (\text{EQ 30})$$

where $1 - D_m$: dissipation of mechanical energy input,
 $1 - D_h$: dissipation of convective energy input.

The dissipation terms are specified according to observations and are depth dependent.

The kinetic energy input is provided by the ice velocity, which is simulated by the ice model:

$$K = \gamma^* C_{do} |v_i|^3, \quad (\text{EQ 31})$$

where γ^* : empirical friction parameter.

Equation (EQ 30) applies only for the deepening of the mixed layer, i.e. $w_e > 0$. During the melting phase the mechanical energy input is usually insufficient to overcome the stabilizing effect of the surface buoyancy flux ($w_e < 0$). In that case, the mixed layer is reduced to an equilibrium depth, which is diagnostically determined by the Monin-Obukhov length from (EQ 30) with $w_e = 0$. The prognostic equations (EQ 22), (EQ 24) and (EQ 25) are then solved with $w_e = 0$ as well.

2.1.3 Atmospheric surface-layer [ASL] parameterization

The parameterization of the atmospheric surface layer used here is similar to the one of the ECMWF model (ECMWF Research Department, 1985) and refers to Louis (1979). It is based on the Monin-Obukhov similarity theory, the Monin-Obukhov length being replaced by the Richardson number of the lowest model (AGCM) level:

$$\text{Ri} = \frac{gz_{a1} [(\theta_{a1} - \theta_s) + 0.61\theta_s (q_1 - q_s)]}{\theta_s |v_{a1}|^2}, \quad (\text{EQ 32})$$

where

- z_{a1} : height of lowest atmosphere layer,
- θ_{a1} : potential temperature of lowest atmosphere level,
- θ_s : potential temperature at the surface ($\approx T_s$),
- q_1 : specific humidity of lowest atmosphere layer,
- q_s : specific humidity at the surface,
- v_{a1} : wind in the lowest atmosphere layer.

In this case the lowest atmosphere level stands for the lowest level of the AGCM (assigned height ≈ 30 m), contrary to the application of Stössel (1991), where z_{a1} rises, if $p_{as} \geq 1004$ hPa.

The friction velocity is given by:

$$V_d = \frac{\kappa}{\ln(z_{a1}/z_s)} |v_{a1}| \sqrt{F'_m}, \quad (\text{EQ 33})$$

where

- κ : von Karman constant,
- z_s : roughness length,
- F'_m : stability function for momentum flux,

and the sensible heat flux by:

$$Q_{se} = -\rho_a c_a \frac{\kappa^2 |v_{a1}| (\theta_{a1} - \theta_s) F'_h}{0.74 \ln^2(z_{a1}/z_s)}, \quad (\text{EQ 34})$$

where F'_h : stability function for turbulent heat flux.

The latent heat flux is given by an analogous formula with q_1 and q_s .

After a slight modification according to Claussen (1991), the stability functions combine as follows:

$$F'_{m,h} = \left[\frac{1}{(1 + 2 \cdot 4.7 \text{ Ri})^2} \right] \delta_{jk} + \left[1 - \frac{9.4 \text{ Ri}}{1 + c_{m,h} |\text{Ri}|^{1/2}} \right] (1 - \delta_{jk}) \quad (\text{EQ 35})$$

where $j = k$, if $\text{Ri} \geq 0$,
with

$$c_{m,h} = (7.4, 5.3) \left[\frac{\kappa}{\ln(z_{a1}/z_s)} \right]^2 9.4 \sqrt{z_{a1}/z_s} .$$

For neutral and unstable stratifications these formulae are derived from an analytical adjustment to the stability functions of Businger et al. (1971). At highly stable stratifications, the fluxes are assumed to approach an asymptote in order to prevent the drag coefficient from being essentially zero.

2.1.4 Atmospheric boundary-layer [ABL] model

By this one-dimensional ABL model, applied earlier by Koch (1986, 1988), the atmospheric forcing level is raised to the geostrophic level, thus including the entire Ekman layer.

The surface (Prandtl) layer is treated similarly to the previous section, i.e. making use of the Monin-Obukhov similarity theory, where

$$L' = -\rho_a c_a \frac{T_s}{g \kappa} \frac{V_d^3}{(Q_{se} + (0.61 T_s c_a Q_{la}) / L_v)} \quad (\text{EQ 36})$$

is the Monin-Obukhov length and L_v is the latent heat of evaporation. The corresponding vertically integrated turbulent heat fluxes are:

$$Q_{se} = -\rho_a c_a \frac{\kappa V_d}{f'_h} (\theta_{a1} - \theta_s) \quad (\text{EQ 37})$$

and

$$Q_{la} = -\rho_a L_v \frac{\kappa V_d}{f'_h} (q_1 - q_s) \quad (\text{EQ 38})$$

and the stress at the surface:

$$|\tau_a| = \rho_a \frac{\kappa V_d}{f'_m} |v_{a1}| \quad (\text{EQ 39})$$

where f'_h and f'_m represent the respective stability functions according to Businger et al. (1971) (see Koch, 1986, page 91 and 92), which are functions of z_{a1}/L' only.

The Rossby number similarity theory yields (after vertical integration) the resistance laws of the barotropic Ekman layer, relating the surface variables to those at the geostrophic level:

$$Q_{se} = -\rho_a c_a \kappa V_d (\theta_{a2} - \theta_s) \left[\ln \frac{V_d}{f z_s} - C(\mu) \right]^{-1} \quad (\text{EQ 40})$$

$$Q_{la} = -\rho_a L_v \kappa V_d (q_2 - q_s) \left[\ln \frac{V_d}{f z_s} - C(\mu) \right]^{-1} \quad (\text{EQ 41})$$

$$\ln \frac{V_d}{|v_{a2}|} = A(\mu) - \ln \frac{|v_{a2}|}{f z_s} + \left[\left(\kappa \frac{|v_{a2}|}{V_d} \right) - B^2(\mu) \right]^{1/2} \quad (\text{EQ 42})$$

where θ_{a2} : potential temperature of the second (geostrophic) atmosphere layer,
 q_2 : specific humidity of the second atmospheric layer,
 v_{a2} : wind in the second atmospheric layer,

and where A , B and C are functions of the stability parameter

$$\mu = \frac{\kappa V_d}{fL'} \quad (\text{EQ 43})$$

(Fiedler and Panofski, 1972, see also Koch, 1986, page 93).

Additionally, the similarity theory of the Ekman layer provides the turning angle between the geostrophic flow and the surface stress:

$$\sin\phi_a = -\frac{B(\mu)}{\kappa} \frac{V_d}{|v_{a2}|} . \quad (\text{EQ 44})$$

Thus, the stress between ice and atmosphere yields:

$$\tau_a = \rho_a V_d^2 \frac{v_{a2}}{|v_{a2}|} \begin{bmatrix} \cos\phi_a & -\sin\phi_a \\ \sin\phi_a & \cos\phi_a \end{bmatrix} . \quad (\text{EQ 45})$$

The application of these laws implies horizontal homogeneity, implicitly assuming the boundary layers to develop separately and non interdependently over ice free and ice covered water.

2.2. FINITE DIFFERENCE FORM

(EXTRACT FROM HIBLER, 1979)

The simultaneous equations (EQ 1), (EQ 3d) and (EQ 4)-(EQ 6) are numerically solved as an initial-value problem using finite-difference techniques on a spatially staggered (Arakawa-B) grid. The spatial finite-difference code is outlined in section 2.2.1 for the momentum equations and in section 2.2.2 for the continuity equations.

For the solution of the momentum equations (EQ 1) a semi-implicit predictor-corrector procedure is used to center the nonlinear terms. Under this procedure two relaxation solutions are required at each time step, one to center the nonlinear terms and one to advance to the next step. In each case point relaxation techniques are used to solve the linearized implicit equations.

The continuity equations (EQ 4)-(EQ 6) are integrated explicitly, with the advection terms integrated by a modified Euler step and the diffusion and thermodynamic terms by a forward Euler step.

This time-marching procedure for the coupled equations can be conveniently illustrated using the simplified one-dimensional equations:

$$\frac{\partial u}{\partial t} = \left(\frac{\partial}{\partial x}\right) \left[\eta(u, P) \frac{\partial u}{\partial x} \right] - D(u) u - \frac{\partial P}{\partial x} - u \left(\frac{\partial u}{\partial x}\right) \quad , \quad (\text{EQ 46})$$

$$\frac{\partial h}{\partial t} = -\frac{\partial}{\partial x}(uh) + f(h) - Dh \quad , \quad (\text{EQ 47})$$

$$P = P(h) \quad , \quad (\text{EQ 48})$$

where, for illustrative purposes, the diffusion term has been replaced by a simple drag term. In time, h is considered to be defined at $t^{i+1/2}$ and u at t^i . To advance u requires two steps (denoting spatial differences by δ_x and time location by superscripts):

$$u^{i+1/2} = u^i + \frac{1}{2}\Delta t \{ \delta_x [\eta(u^i, P^{i+1/2}) \delta_x u^{i+1/2}] - D(u^i) u^{i+1/2} - \delta_x P^{i+1/2} - u^i \delta_x u^{i+1/2} \} \quad (\text{EQ 49})$$

$$u^{i+1} = u^i + \Delta t \{ \delta_x [\eta(u^{i+1/2}, P^{i+1/2}) \delta_x u^{i+1}] - D(u^{i+1/2}) u^{i+1} - \delta_x P^{i+1/2} - u^{i+1/2} \delta_x u^{i+1} \} \quad (\text{EQ 50})$$

where both equations are solved for the u 's by relaxation. Note that (EQ 49) provides an estimate of $u^{i+1/2}$ for the use in the nonlinear terms in the basic timestep (EQ 50). Once the velocity has been advanced to time t^{i+1} the thickness is then advanced by the two-step procedure, i.e.,

$$h^{i+3/2*} = h^{i+1/2} - \Delta t \delta_x (u^{i+1} \cdot h^{i+1/2}) \quad , \quad (\text{EQ 51})$$

$$h^{i+3/2} = h^{i+1/2} - \Delta t \left\{ \delta_x \left[u^{i+1} \cdot \frac{1}{2} (h^{i+1/2} + h^{i+3/2*}) \right] - D h^{i+1/2} + f(h^{i+1/2}) \right\} \quad (\text{EQ 52})$$

The first equation in this modified Euler procedure provides a provisional value in order to approximately center the advection term in the second equation. Note that since h and u are staggered in time the coupled system is effectively being integrated by the efficient forward-backward scheme (Mesinger and Arakawa, 1976).

2.2.1 Momentum equations

In the momentum equations it is necessary to solve by relaxation coupled linearized equations with Dirichlet boundary conditions of the form:

$$\lambda v + D_a v - D_s u + F_x + A_1 \frac{\partial u}{\partial x} + A_2 \frac{\partial u}{\partial y} = \tau_x \quad , \quad (\text{EQ 53})$$

$$-\lambda u - D_s v - D_a u + F_y + A_1 \frac{\partial v}{\partial x} + A_2 \frac{\partial v}{\partial y} = \tau_y \quad , \quad (\text{EQ 54})$$

where $\lambda, D_a, D_s, A_{1,2}$ are spatially varying constants, F_x and F_y are given by (EQ 3) and τ_x and τ_y are input forcing fields. To obtain finite-difference forms of F_x and F_y expressions are needed for terms of the form $(\eta u_x)_x, (\eta u_y)_x, (\eta u_y)_y, (\eta u_x)_y, P_y, P_x$ and similar terms with u replaced with v . (In these expressions x and y subscripts indicate spatial finite differences.) To show the general format it suffices to illustrate the 1st two terms and the last term. Denoting space coordinates by subscripts and using half-integer subscripts for η and P since a staggered grid is employed, the following forms were used for a square grid with mesh size h :

$$\begin{aligned} \{(\eta u_x)_x\}_{ij} = \frac{1}{2h^2} [& (\eta_{i+1/2, j-1/2} + \eta_{i+1/2, j+1/2}) (u_{i+1, j} - u_{i, j}) \\ & - (\eta_{i-1/2, j-1/2} + \eta_{i-1/2, j+1/2}) (u_{i, j} - u_{i-1, j})] \quad , \end{aligned} \quad (\text{EQ 55})$$

$$\begin{aligned} \{(\eta u_y)_x\}_{ij} = \frac{1}{4h^2} [& (\eta_{i+1/2, j+1/2}) (u_{i+1, j+1} + u_{i, j+1} - u_{i+1, j} - u_{i, j}) \\ & + (\eta_{i+1/2, j-1/2}) (u_{i+1, j} + u_{i, j} - u_{i+1, j-1} - u_{i, j-1}) \\ & + (\eta_{i-1/2, j+1/2}) (u_{i, j} + u_{i-1, j} - u_{i, j+1} - u_{i-1, j+1}) \\ & + (\eta_{i-1/2, j-1/2}) (u_{i, j-1} + u_{i-1, j-1} - u_{i, j} - u_{i-1, j})] \quad , \end{aligned} \quad (\text{EQ 56})$$

$$\{P_x\}_{ij} = \frac{1}{2h} (P_{i+1/2, j+1/2} + P_{i+1/2, j-1/2} - P_{i-1/2, j+1/2} - P_{i-1/2, j-1/2}) \quad . \quad (\text{EQ 57})$$

Denoting by $(F_{xD})_{ij}$ the finite difference expression for F_x with the diagonal components u_{ij} removed with coefficient D_x (and similarly for $(F_{yD})_{ij}$, the expression for F_y with v_{ij} components - coefficient D_y - removed), the finite difference equations are solved at each grid point for the superscripted values in terms of the old i values according to:

$$\lambda v_{ij}^{i+1} + D_a v_{ij}^{i+1} - D_s u_{ij}^{i+1} + (F_{yD})_{ij}^i + D_x u_{ij}^{i+1} + (Au)_{ij}^i = \tau_x, \quad (\text{EQ 58})$$

$$-\lambda u_{ij}^{i+1} - D_s v_{ij}^{i+1} - D_a u_{ij}^{i+1} + (F_{yD})_{ij}^i + D_y v_{ij}^{i+1} + (Av)_{ij}^i = \tau_y, \quad (\text{EQ 59})$$

where $(Au)_{ij}^i$ denotes the momentum advection term

$$\frac{1}{2h} [A_1 (u_{i+1,j}^i - u_{i-1,j}^i) + A_2 (u_{i,j+1}^i - u_{i,j-1}^i)]$$

and similarly for $(Av)_{ij}^i$. The solved equations are then used to replace the old values at position i,j and the sweep continued. Note that at each grid point two simultaneous equations for u_{ij}^{i+1} and v_{ij}^{i+1} must be solved. Without treating the Coriolis terms in this manner the iteration can be shown by a local stability analysis to be unstable for long wavelengths. For an overrelaxation which will normally be faster (but in certain cases can diverge) the old value is replaced by:

$$u_{ij}^1 = w (u_{ij}^{i+1} - u_{ij}^i) + u_{ij}^i$$

and similarly for v_{ij} , where w denotes the relaxation factor (WT).

The only other finite differences needed for the momentum equations are strain rate estimates for use in calculating the nonlinear viscosities. These were obtained by an average over the grid cell, e.g. :

$$(\dot{\epsilon}_{11})_{i+1/2,j+1/2} = \frac{1}{2h} [u_{i+1,j+1} + u_{i+1,j} - u_{i,j+1} - u_{i,j}] \quad (\text{EQ 60})$$

with similar expressions for the other components.

2.2.2 Continuity equations

In the ice thickness equations spatial finite difference of the following terms is required to explicitly integrate the equations forward in time:

$$\frac{\partial}{\partial x}(uh), \frac{\partial}{\partial y}(vh), D_1 \frac{\partial^2 h}{\partial x_i^2}, D_2 \frac{\partial^4 h}{\partial x_j^2 \partial x_i^2} \quad . \quad (\text{EQ 61})$$

For the advection terms, spatial differences of the following form are employed, *viz.*,

$$\begin{aligned} [(uh)_x]_{i+1/2, j+1/2} = & \frac{1}{4h} [(h_{i+1/2, j+1/2} + h_{i+3/2, j+1/2})(u_{i+1, j+1} + u_{i+1, j}) \\ & - (h_{i+1/2, j+1/2} + h_{i-1/2, j+1/2})(u_{i, j+1} + u_{i, j})] \end{aligned} \quad (\text{EQ 62})$$

and similar for $(vh)_y$. Since the velocities are zero at the boundaries this automatically conserves mass and can be shown to conserve energy for the incompressible portion of the velocity field. In order to conserve mass for the diffusion terms, the diffusion coefficients are considered to be spatially varying - zero on the boundaries and constant in the interior. The harmonic diffusion term for example is thus properly written

$$\left(\frac{\partial}{\partial x_i} \right) / \left[D_1 \left(\frac{\partial h}{\partial x_i} \right) \right] \quad (\text{EQ 63})$$

and in finite-difference form is (where for convenience the half integer subscripts have been replaced by integers for the h 's):

$$\{ (D_1 h_x)_x \}_{ij} = \{ (h_{i+1, j} - h_{i, j}) D_{1i+1/2, j} - (h_{i, j} - h_{i-1, j}) D_{1i-1/2, j} \} \quad (\text{EQ 64})$$

with a similar expression for $(D_1 h_y)_y$. For the biharmonic diffusion term, it is considered to be of the form

$$\frac{\partial}{\partial x_l} \sqrt{D_2} \frac{\partial}{\partial x_l} \frac{\partial}{\partial x_p} \sqrt{D_2} \frac{\partial h}{\partial x_p} \quad (\text{EQ 65})$$

and is performed by two successive harmonic diffusion operations.

2.3. MODEL DEVELOPMENT

The dynamic-thermodynamic sea-ice model developed by Hibler (1979) was originally designed for the Arctic Ocean. After having been extended by explicit calculation of the heat balance, the model was applied to the Weddell Sea region (Hibler and Ackley, 1983). This version was later modified by Hibler (1984) to include creation of extra open water due to shear deformation for the ice compactness equation and a seven-level ice thickness distribution for the calculation of the heat balance over the ice covered part of a grid cell. Thus modified, the model has been supplemented to include a prognostic snow layer (Owens and Lemke, 1990), and has been coupled to the OML model of Lemke (1987) (Lemke et al., 1990). Finally, this upgraded model system has been geographically extended to the entire Southern Ocean region (Stössel et al., 1990). For internal technical purposes this model version was called “cycle 4”.

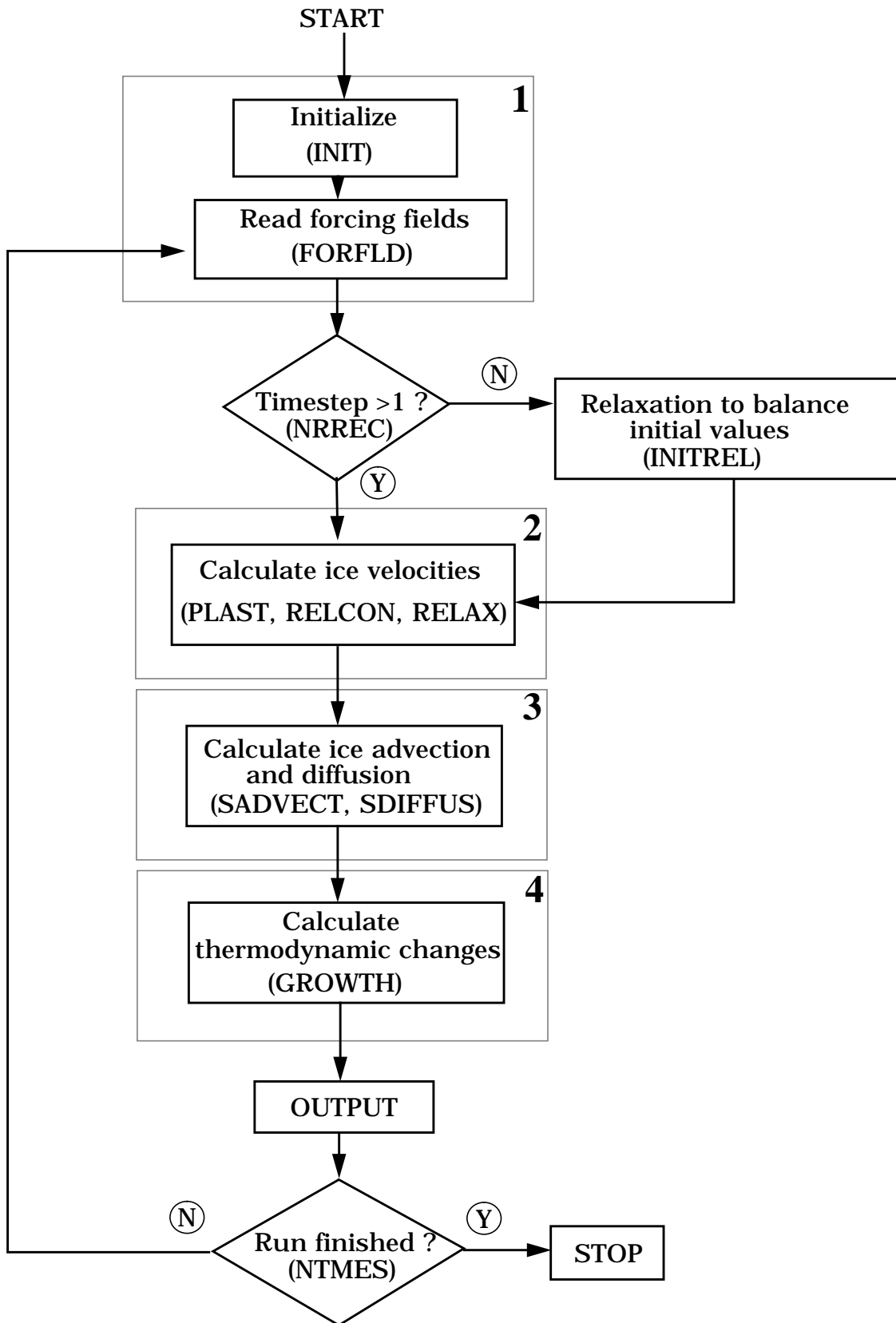
Independent from this evolution, the Weddell Sea-ice model version from Hibler and Ackley (1983) has been coupled to an ABL model by Koch (1986, 1988). Coupling of this ABL model to the upgraded and extended model version mentioned above (cycle 4) and using the same monthly mean, climatological atmospheric forcing as described in Stössel et al. (1990), yielded the version cycle 5.

Starting with cycle 6, the atmospheric forcing in terms of temperature, humidity, surface pressure and wind consisted of daily values from the ECMWF global analyses. The following cycles differ with respect to the treatment of the atmospheric boundary layer: cycle 6 including the entire ABL (Prandtl + Ekman layer) with forcing from the geostrophic level, cycle 7 being the same as cycle 6 except that the wind forcing is taken from the lowermost analyses level and the friction velocity determined by the surface layer formulation.

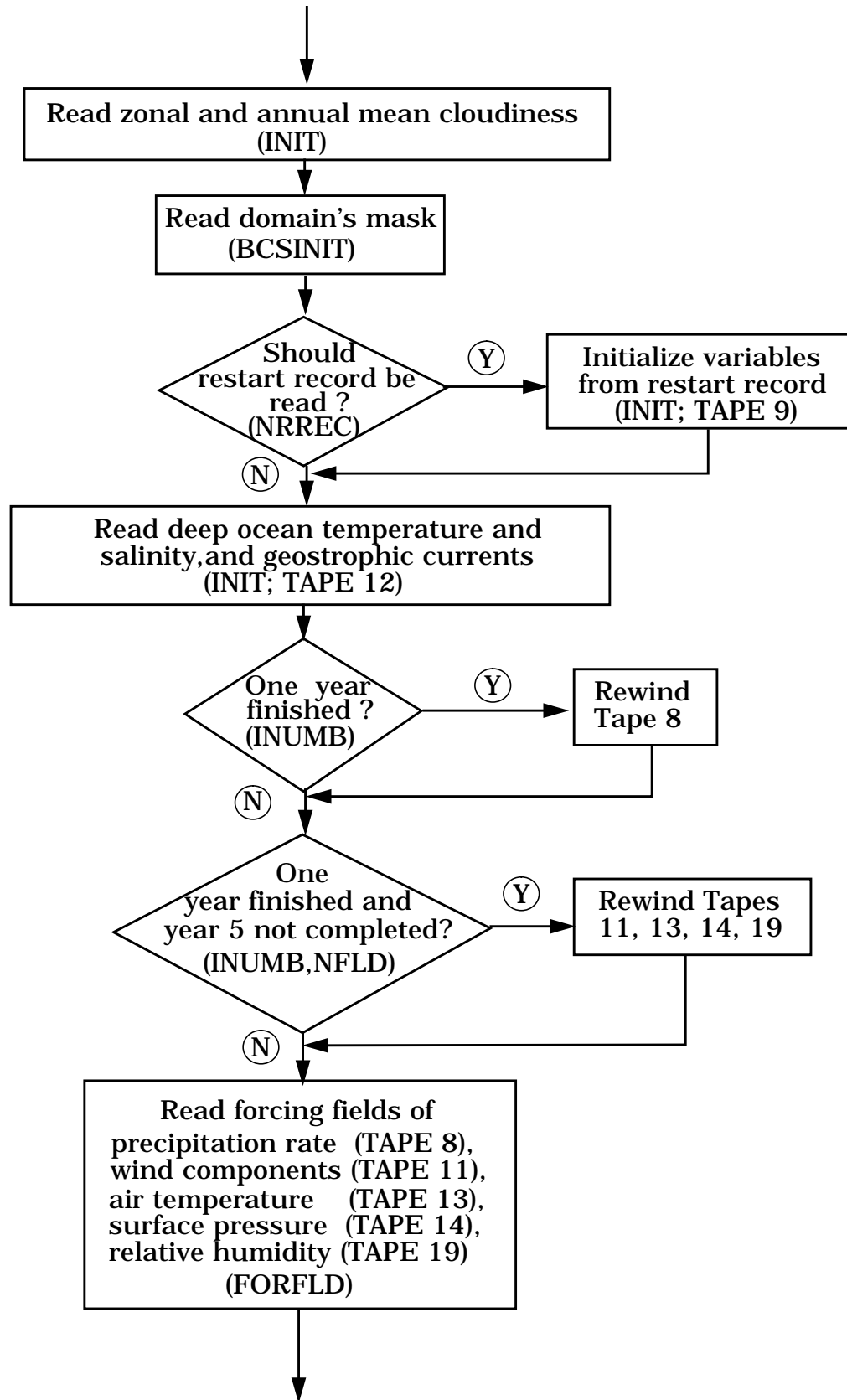
In cycle 8 the atmospheric forcing is applied at the surface without any boundary layer treatment. Cycle 9 and 10 were designed for specific test experiments not being of interest in the present context. Cycle 11, the current application, employs the ASL parameterization, where the atmospheric forcing is essentially given by the 1000 hPa field of the analyses (Stössel, 1991).

3. SYSTEM DESCRIPTION

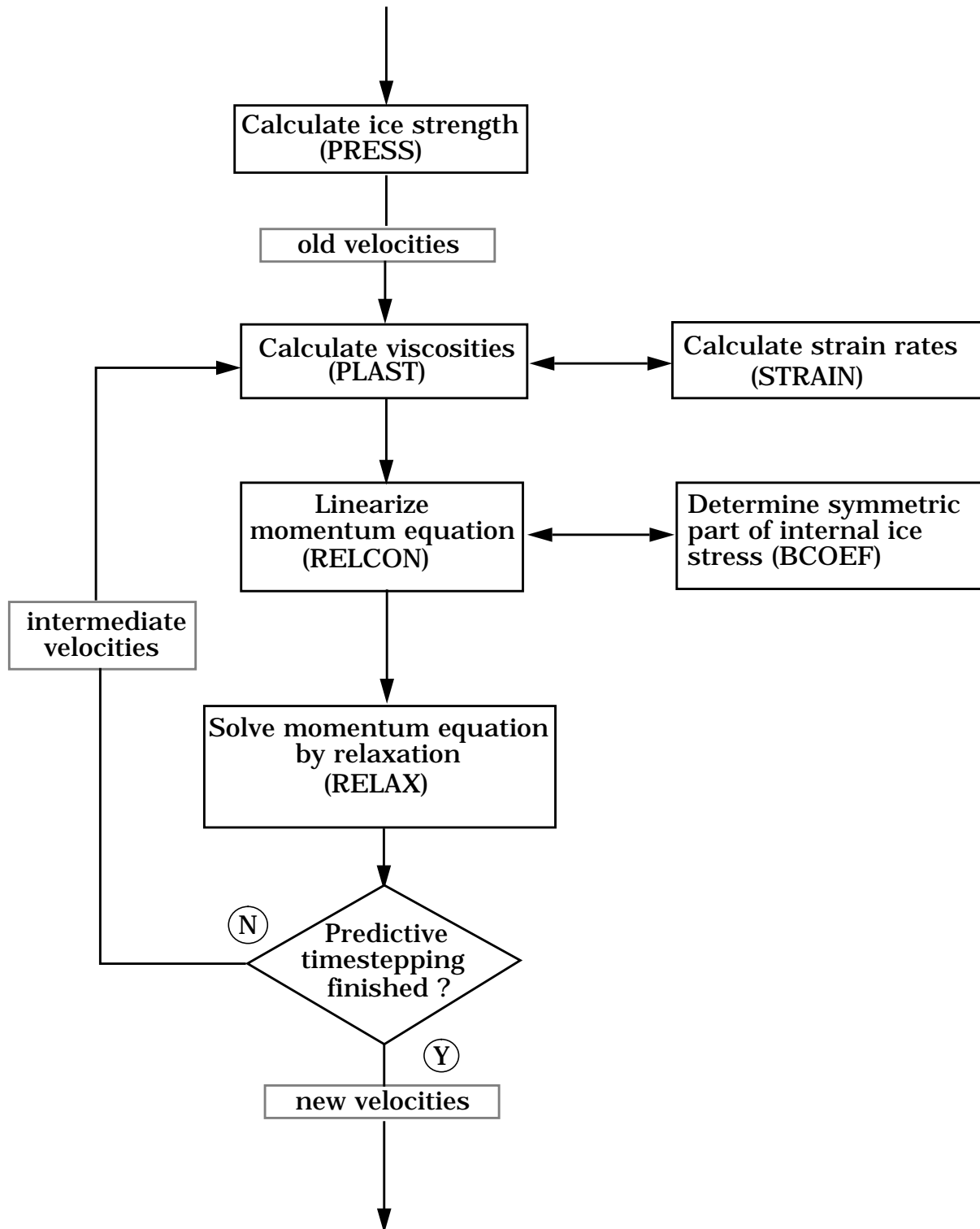
3.1. FLOW DIAGRAM



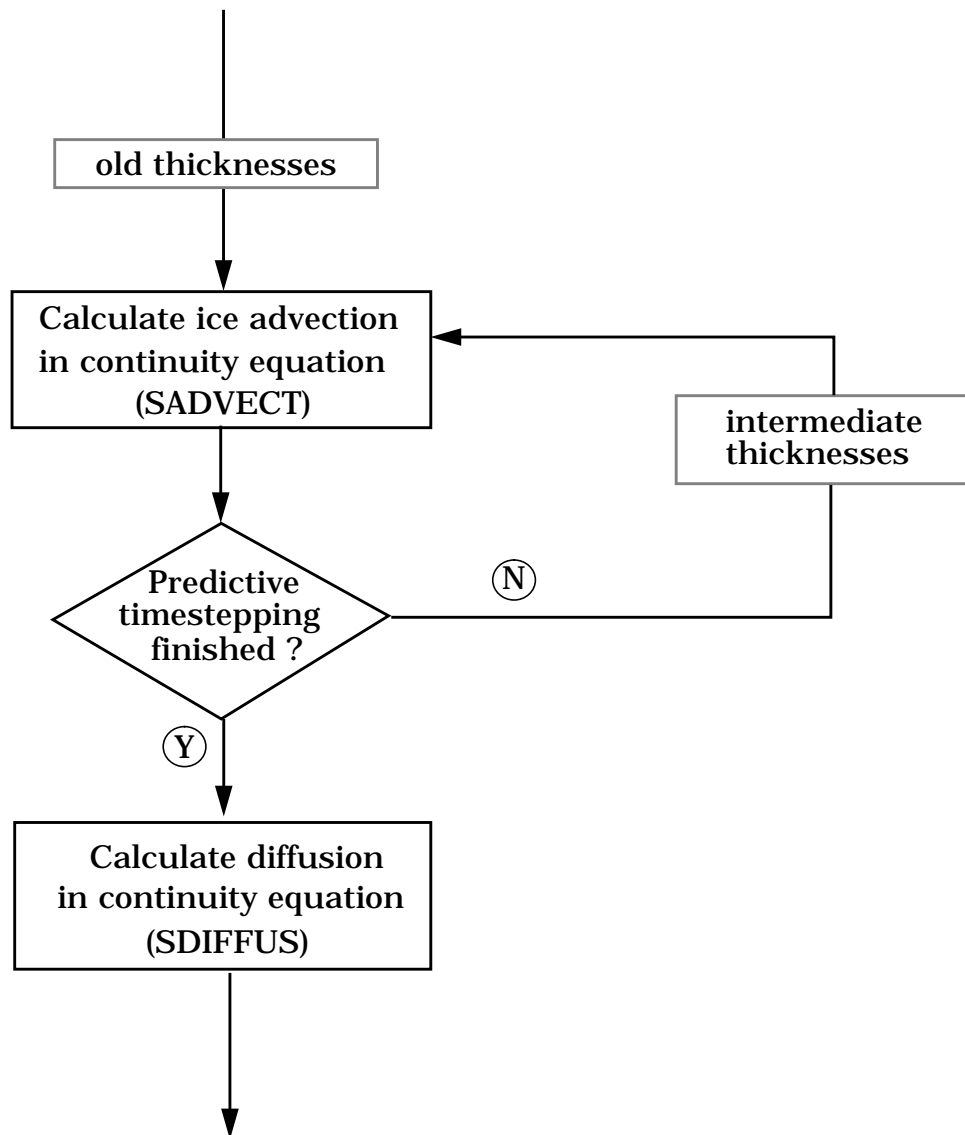
1 Initialisation and reading of forcing fields



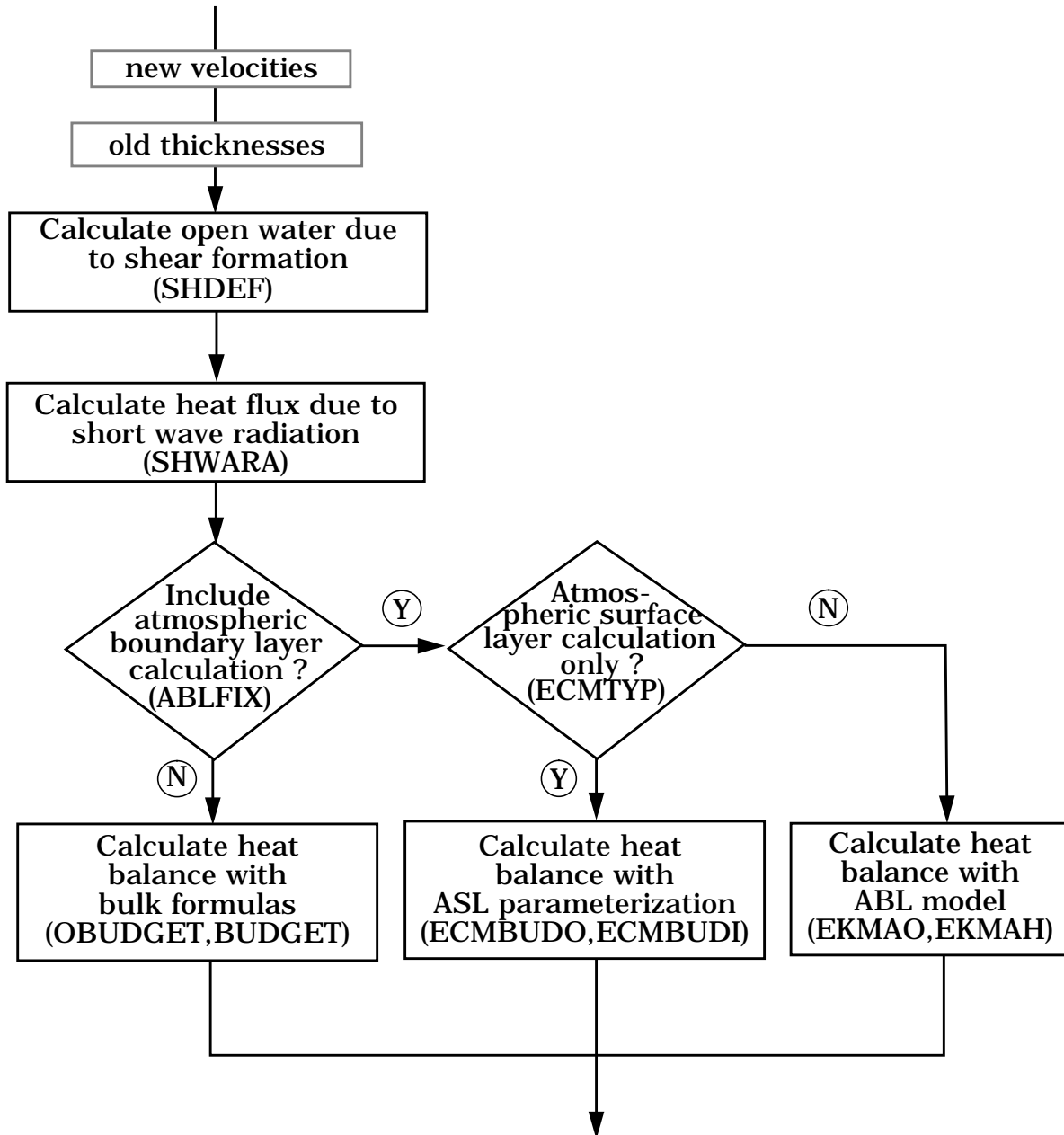
2 Calculation of ice velocities



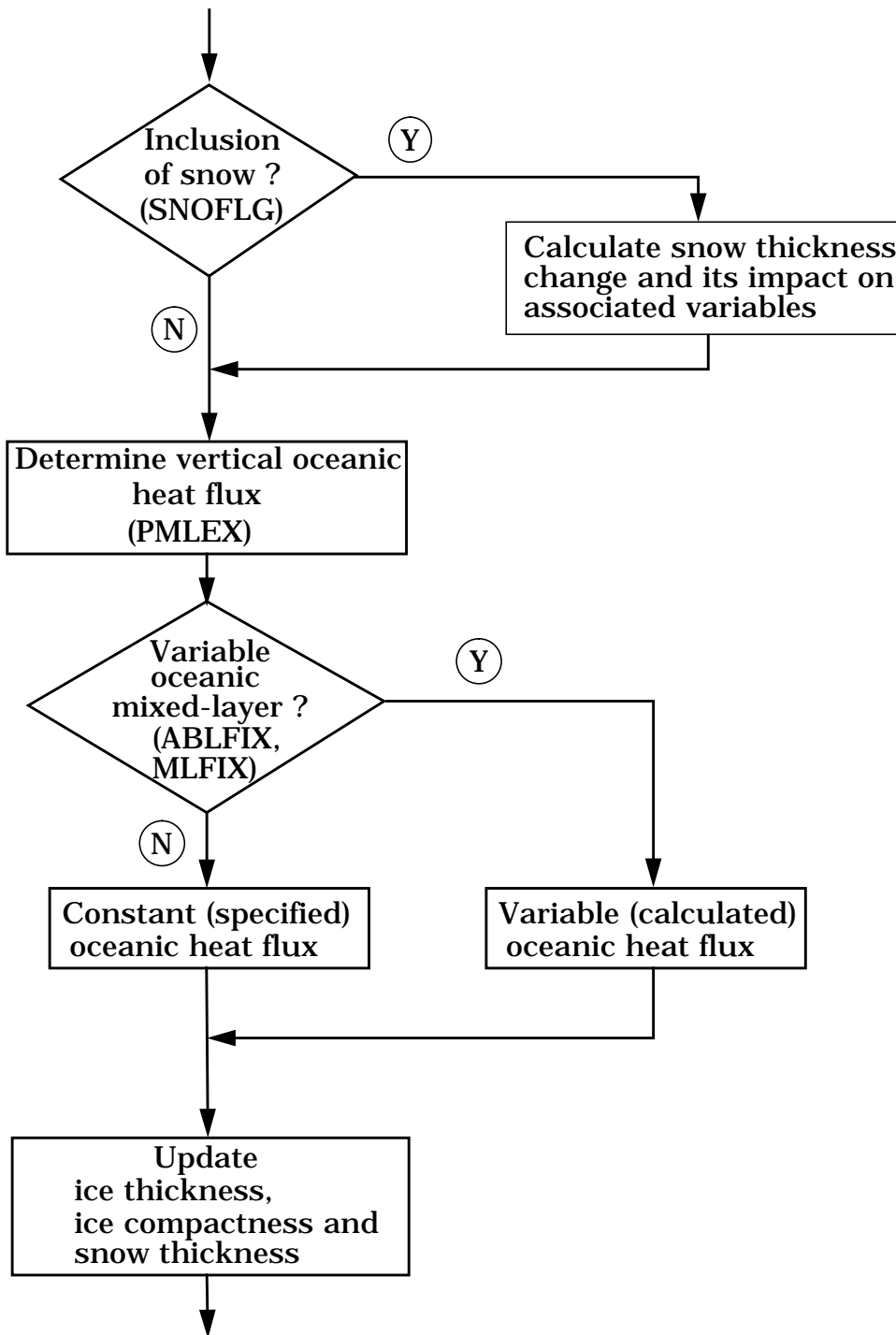
3 Calculate ice advection and diffusion



4 Calculation of thermodynamic changes



4 Calculation of thermodynamic changes (continued)



3.2. DESCRIPTION OF IMPORTANT ROUTINES

The important routines are:

Dynamic part

PRESS: calculates the ice strength

PLAST: calculates viscosities

STRAIN: calculates strain rate tensor

RELCON: linearizes the momentum equation

RELAX: solves momentum equation

SADVECT: calculates ice advection

SDIFFUS: calculates diffusion

Thermodynamic part

GROWTH: calculates thermodynamic changes

BUDGET: solves heat balance with bulk formulas

ECMBUDI: solves heat balance with the ASL parameterization

EKMAH: solves heat balance with the ABL model

PMLEX: calculates changes in oceanic mixed layer

3.2.1 Details of the important routines

Dynamic part

PRESS:

Calculates the ice strength according to (EQ 3d). Uses ice thickness and compactness at the old time step. P^* (PSTAR) and C^* (CSTAR) are empirical constants specified in INIT.

PLAST:

Calculates bulk and shear viscosities according to (EQ 3b) and (EQ 3c). Uses the strain rates calculated in STRAIN for the determination of the strain rate invariants (EQ 3e) and uses the ice strength previously determined in PRESS.

STRAIN:

Calculates the strain rate tensor following eq. (A5) in Leppäranta and Hibler (1985). Determines the strain rates at the grid center points by first interpolating to half way between the grid edge points, and then differentiating, using the old velocities for the centering time step and the intermediate ones for the advancing time step.

RELCON:

The equations partially treated in this routine are (EQ 1)-(EQ 3). Extracts those parts of the momentum equation that do not depend on the velocities of the current time step (FX,FY). Provides the symmetric (BU,BV) and asymmetric (ASY) coefficients for the velocities at the new time step (to be solved in RELAX). Uses the old ice thicknesses for the determination of the ice mass, the old pressure (ice strength) for the force due to internal ice stress, the old velocities for the contribution of the local rate of change from the old time step and, optionally, the calculated air/ice drag coefficient and turning angle of the old time step. Otherwise, the old or intermediate ice velocities are used.

RELAX:

Calculates the ice velocities by solving that part of the momentum equation that depends on the velocities of the current time step. This requires a relaxation procedure, which is described in section 2. Specifically, the solution is obtained by a semi-implicit predictor corrector procedure, requiring two relaxation solutions per time step, i.e. one to center the non-linear terms and one to advance to the next time step. The time-marching procedure is illustrated by (EQ 46)-(EQ 50). In the code, the current time step is indicated by index LN, while LR indicates the previous time step. The spatial finite-difference pattern for the momentum equations is illustrated in section 2.2.1. Specifically, we are solving the linearized equations:

$$BU \cdot U - ASY \cdot V = RU + FX$$

$$BV \cdot V + ASY \cdot U = RV + FY$$

where

BU,BV:	symmetric coefficients,
U,V:	instantaneous velocities,
ASY:	asymmetric coefficient,
RU,RV:	terms independent of values at local grid point,
FX,FY:	terms independent of values at current time step.

Taking the reciprocal of the symmetric coefficients (BU,BV) at the end of RELCON and solving for the ice velocities (U,V) yields:

$$U - (ASY \cdot BU) \cdot V = (RU + FX) \cdot BU$$

$$V + (ASY \cdot BV) \cdot U = (RV + FY) \cdot BV$$

which finally is solved by the relaxation procedure.

SADVECT:

Calculates the advection of a scalar variable for the continuity equations (EQ 4) - (EQ 6). It employs centered differences in space according to section 2.2.2, and a forward-backward (Matsuno) scheme according to Mesinger and Arakawa (1976) and as illustrated by (EQ 51) and (EQ 52). In the code, the latter is provided by using the old scalar variables for the first time through, and an update (intermediate time step) of these variables for the second time through, both indicated by the index LRHS.

SDIFFUS:

Calculation of diffusion of a scalar variable for the continuity equations (EQ 4) - (EQ 6). It employs a forward (Euler) scheme for time integration, using the old scalar variables. Uses harmonic and biharmonic diffusion terms according to (EQ 63) - (EQ 65), thus making the diffusion coefficients spatially variable.

Thermodynamic part

GROWTH:

Calculates changes in ice thickness, ice compactness and snow thickness due to thermodynamic effects according to (EQ 15)-(EQ 17). Includes the calculation of creation of extra open water due to shear deformation (SHDEF) shown in (EQ 7), using the new strain rates. Includes the routine for the calculation of incoming short wave radiation (SHWARA). Calls the heat budget routines for the open water and ice covered part of a grid cell (optionally provided with atmospheric boundary layer formulations). For the latter, the appropriate albedo and effective ice thickness (optionally modified for the seven-level ice thickness distribution) is provided. Subsequently (optionally), the snow thickness is changed by precipitation and melt, and variables influenced by this change are updated. The ice thickness, ice compactness and snow thickness are updated to include the effects of the vertical oceanic heat flux, which is (optionally) calculated in the oceanic mixed-layer routine (PMLEX). Finally, snow is converted to ice whenever the draft of the ice-plus-snow column exceeds the ice thickness.

BUDGET:

Calculation of growth rates for ice covered part of a grid cell with standard bulk formulas. First, the surface temperature of ice (or snow) is calculated by iteratively solving the heat balance equation (EQ 8) using the old “effective” ice thickness (EQ 10). For the iteration procedure the “regula falsi” method has been used instead of the more common “Newton-Raphson” method in order to be commensurate with the method used in the ABL-routines. For the same reason, the intermediate storage of variables into a one-dimensional array has been adopted (making no computational sense in the present routine). Using the new surface temperature, the atmospheric contribution to the ice growth rate at the bottom (FHB) is determined by the updated conductive heat flux. In case of positive surface temperatures, these are set to zero and implemented into the heat balance equation in order to achieve the ice melt rate at the surface (FHI).

ECMBUDI:

Calculates ice growth rates for ice covered part of a grid cell with ASL parameterization based on the Monin-Obukhov theory according to Louis (1979) illustrated in section 2.1.3. The overall structure of the present routine in terms of the iteration procedure and the growth rate calculation, is similar to BUDGET. The essential difference occurs due the fact that the turbulent heat fluxes (FLSE and FLLA,(EQ 34)) are now dependend on stability functions ((EQ 35) determined in RISTAB), which themselves are functions of the Richardson number (TMPL, (EQ 32)) and the (specified) roughness length (ZOI). Finally, a stability dependent drag coefficient (to be used in RELCON for the subsequent time step) is determined via the friction velocity (UST, (EQ 33)).

EKMAH:

Calculates ice growth rates for the ice covered part of a grid cell with the ABL model presented in section 2.1.4, which is essentially based on the resistance laws of the barotropic Ekman layer (Koch, 1986,1988), thus employing Rossby number similarity theory with atmospheric forcing from the geostrophic level ((EQ 40)-(EQ 45)). To determine the variables of the atmospheric surface layer, Monin-Obukhov theory has been applied ((EQ 36)-(EQ 39)). The non-linear system of equations is solved by three iteration procedures, namely for the surface temperature (T), the stability parameter (WMUE) and the friction velocity (UST). Since the iteration procedures can be computationally time consuming, especially when the seven-level ice thickness formulation is employed, the code has been optimized to continue the iterations only in those grid cells, where the currently achieved solution does not satisfy the specified truncation. This procedure requires an intermediate storage of the variables of the instantaneously involved grid cells into a one-dimensional array. After a satisfying solution is found for all three iteration variables, the procedure is repeated using the updated variables (“overall iteration loop”). This overall iteration is repeated until the overall truncation limit (TMYUS) is achieved. To yield the correct spatial distribution for the final calculation of the growth rates, the currently involved variables in the one-dimensional array are “unscrambled” (tranferred back into the two-dimensional array) after each overall iteration time step. The present routine calls the routines STAB and RESIST for the calculation of the stability functions of the Prandtl layer (PH1,PH2) and the Ekman layer (A,B,C), respectively.

PMLEX:

Calculation of oceanic mixed-layer variables according to the OML model of Lemke (1987) presented in section 2.1.2 updates heat and salt content of the water column ((EQ 19)-(EQ 21)), including a parameterization of advective effects by Newtonian coupling of the salinities to observations (Lemke et al.,1990). In the case of fixed mixed layer (MLFIX=1), temperature and salinity of the mixed layer are computed using a constantly specified oceanic heat flux (QTOC). In the case of mixed-layer retreat (IEN=0), the new mixed-layer depth exponentially decays to the Monin-Obukhov length. The time constant for this is given by RTC and is set in INIT (present value = 10 days). Otherwise, the entrainment velocity is calculated according to (EQ 30). After updating the mixed-layer and the pycnocline variables using the new entrainment velocity ((EQ 21)-(EQ 25)), vertical diffusion is introduced if the thermocline or the halocline thicknesses become less than 5 m (VERDIF). Subsequently, the mixed-layer heat storage and the ice thickness are adjusted in order to keep the mixed-layer temperature at the freezing point as long as ice is present in a grid cell (ADJUEX). Finally, convective overturning is provided for the case of unstable stratification.

4. USER'S MANUAL

4.1. RUNNING THE MODEL

4.1.1 Batchfile to run the model

An example of a UNICOS batch job started from the Cray-2S is given in App.B. After compiling and loading, the domain's mask (mask) and the forcing fields (tsuvwg, prj, uve, tae, rhe and pae) are assigned, the code being ready for start. The files fort.15-fort.18 and fort.20 are reserved for the output, CJOBOUT being assigned for control output.

4.1.2 Script for running the model

Changing the source code of the SUBROUTINE, whose name follows "->", you should be able to create the same computation results as shown in App.C:

-choose the number of time steps for model integration:

-> INIT: NTMES = 30 (= 30 days)

-choose interval for statistics output:

-> INIT: NSTAT = 1 (= at each time step)

-choose interval for spatial pattern outputs (as integers):

-> INIT: NSTA = 15 (= every 15th time step, starting with
(IIC-5) => output at day 10 and 25)

-decide after which step to begin with any outputs:

-> INIT: NFLD = 0 (= from the very beginning)

-choose interval for plot outputs:

-> INIT: NPLT = 90 (= every 90th time step, starting with
(IIC-5) => output at day 85, 175 etc., i.e.
no output in the present example)

-decide about reading or writing restart records:

-> INIT: NRREC, NRST (not used in the present code)

-choose the cycle according to the header info:

-> INIT:	ABLFIX = 0	(= variable ABL)	} = cycle 11
-> INIT:	SURFWIN = 1	(= no wind turning)	
-> INIT:	ECMTYP = 1	(= ASL model)	

-decide about consideration of snow:

-> INIT: SNOFLG = 1 (= with snow)

-decide about having a variable or fixed OML:

-> INIT: MLFIX = 0 (= variable OML)

-decide about which spatial patterns to plot:

-> ICEMODEL: CALL DRUCKF

4.1.3 Standard diagnostic output

The standard output shown in App.C is mostly self-explaining. The spatial patterns are oriented upward to the north and rightward to the east, starting at the upper left corner with $\varphi = 51.25^\circ \text{ S}$ and $\lambda = 2.5^\circ \text{ E}$ for the scalar variables and with $\varphi = 52.5^\circ \text{ S}$ and $\lambda = 5^\circ \text{ E}$ for the vector variables, showing every second grid point in zonal direction (spacing: 10°) and each grid point in meridional direction (spacing: 2.5°).

4.2. PREPROCESSING

4.2.1 List of input data sets

<u>Permanent</u> <u>filename</u>	<u>Fortran</u> <u>Unit No.</u>	<u>Contents</u>
mask	10	geographical definition patterns of domain
tsuvwg	12	annual temperature and salinity at 500 m depth, and geostrophic currents
prj	8	monthly precipitation
uve	11	daily wind components
tae	13	daily temperature
rhe	19	daily relative humidity
pae	14	daily surface air pressure

4.2.2 Details of input data sets

mask:

The definition array of the domain consists of three masks as shown below, in particular of the “velocity” mask (VM) for the vector variables at the grid edge points and the “thickness” mask (OM) for the scalar variables at the grid center points. The third mask (HM) is identical to OM, except for the outflow grid cells (in this case at the northern boundary at 50° S). As indicated in the print of the masks (App. D), the reading of the masks (as well as all other input data files) start at the southern boundary, continuing to the east and to the north. Note that the first and last actual grid points in zonal direction (near the seam at $\lambda = 0^{\circ}$) are $I=2$ and $I=73$ in both VM and OM. In meridional direction VM starts with $J=3$ and OM with $J=2$ both ending with $J=12$. This structure occurs due to the staggered nature of the grid and the no slip condition.

tsuvwg:

These data were derived from the Southern Ocean grid point data set of Gordon and Baker (1982), consisting of annual mean values with a horizontal resolution of $1^{\circ} \times 2^{\circ}$. The geostrophic currents were calculated via the dynamic topography, which is itself derived from the density stratification of the upper 1000 m (Stössel et al., 1990). Finally, the temperature [C], salinity [ppt] and currents [m/s] were spatially interpolated to the model grid. The original data set was received from Wenzel at the Alfred-Wegener-Institut, Bremerhaven and is now archived by Jessel, MPI, Hamburg.

prj:

This file contains monthly climatological precipitation data [mm/month] from the grid point data set of Jaeger (1976), originally described on a $5^{\circ} \times 5^{\circ}$ horizontal grid. The monthly mean data were linearly interpolated in time for the one-day time step of the model, assuming the midmonth value to be that of the monthly mean. The present “30-day” extraction essentially represents the January climatology. The original data set was received from Schlese at MI, Hamburg and was recently archived by Jessel, MPI.

uve:

This and the next three files are derived from the twice daily computations of the global analyses of the ECMWF, representing January 1985. The twice daily values were averaged to daily values in order to match with the model time step, and spatially interpolated from the $2.5^{\circ} \times 2.5^{\circ}$ horizontal grid to the model grid. The original computations were made available by DWD, Offenbach and preprocessed by Schnur, MPI. The present file contains the wind components [m/s] at 1000 hPa.

tae:

Represents the surface (2 m) air temperature [C] determined from the 1000 hPa temperatures of the ECMWF analyses by linear vertical interpolation or lapse rate formulation, respectively. Since these computations are approximately equivalent to the potential temperature of the lowest AGCM level of the ECMWF model (≈ 30 m) in the case where the 1000 hPa level is below this level, they are also used as “lowest AGCM level” forcing in the version with ASL parameterization (Stössel, 1991). Otherwise see description of file **uve**.

rhe:

Represents the surface (2 m) relative humidity [%] derived from the 1000 hPa humidities by linear interpolation. Otherwise see description of files **tae** and **uve**.

pae:

(Sea-) Surface pressure [hPa] calculated using the 1000 hPa temperature and humidity as well as the geopotential heights of 850 hPa and 1000 hPa according to Trenberth and Olson (1988). Otherwise see description of file **uve**.

4.3. POSTPROCESSING

4.3.1 List of output data sets

<u>Local</u> <u>file name</u>	<u>Permanent</u> <u>file name</u>	<u>Contents</u>
control.out	CJOBOUT	standard control output
fort.16	SISTA	output of statistics and spatial patterns
fort.18	SISUM	plot output for seasonal cycles
fort.15	SIUV	plot output for vector variables
fort.17	SIISO	plot output for scalar variables
fort.20	SINIM	plot output for selected dates

4.3.2 Details of output data sets

- control.out: Illustrates essential constants of the current model version and prints statistics in terms of integrated variables (e.g. ice volume, ice extent, snow volume).
- fort.16: Additionally to the quantities shown in control.out, this file demonstrates the spatial patterns of various variables (FORMAT: I3) indicated in the respective headlines, an example of which is shown in App.C.
- fort.18: Provides the integrated quantities for the plots of seasonal cycles (FORMAT: 5F8.4).
- fort.15: Provides the components for vector plots, e.g. ice velocities, ocean currents, air/ice stress (FORMAT: 13E10.3).
- fort.17: Contains scalar variables for isoline plots, e.g. ice thickness, ice compactness, temperature, OML thickness (FORMAT: 13E10.3).
- fort.20: Contains computations of ice compactness for specific dates (FORMAT: 13E10.3).

5. REFERENCES

- Businger, J.A., J.C. Wyngaard, Y. Izumi and E.F. Bradley (1971): Flux profile relationships in the atmospheric surface layer. *J. Atm. Sci.*, 28, 181-189.
- Claussen, M. (1991): Local advection processes in the surface layer of the marginal ice zone. *Bound. Layer Met.*, 54, 1-27.
- ECMWF Research Department (1985): Research manual 3, ECMWF forecast model, physical parameterization. *ECMWF Met. Bull.*, M1.6/2(1), Rev. 1.
- Fiedler, F. and H.A. Panofsky (1972): The geostrophic drag coefficient and the effective roughness length. *Quart. J. Roy. Met. Soc.*, 98, 213-220.
- Gordon, A.L. and T. Baker (1982): Objective contouring and the grid point data set. In: *Southern Ocean Atlas*, Columbia University Press, New York, 2, 15-29.
- Hibler, W.D., III (1977): A viscous sea ice layer as a stochastic average of plasticity. *J. Geophys. Res.*, 82(27), 3932-3938.
- Hibler, W.D., III (1979): A dynamic thermodynamic sea ice model. *J. Phys. Oceanogr.*, 9, 815-846.
- Hibler, W.D., III (1980): Documentation for a two-level dynamic-thermodynamic sea ice model. CRREL, Hanover, NH, Special Report, 80-8.
- Hibler, W.D., III (1984): The role of sea ice dynamics in modeling CO increases. In: *Climate Processes and Climate Sensitivity*, eds.: J.Hansen and T.Takahashi, *Geophys. Monogr.*, 29, 238-253.
- Hibler, W.D., III and S.F. Ackley (1983): Numerical simulation of the Weddell Sea pack ice. *J. Geophys. Res.*, 88, 2873-2887.
- Jaeger, L. (1976): Monatskarten des Niederschlages für die ganze Erde. *Berichte des Deutschen Wetterdienstes*, 139.
- Koch, C. (1986): Numerische Simulation der Wechselwirkungen zwischen Meereis und Atmosphäre im Bereich der Weddellsee. Meteorologisches Institut der rheinischen Friedrich-Wilhelms Universität, Bonn, Dissertation.
- Koch, C. (1988): A coupled sea ice- atmospheric boundary layer model, part I: description of the model and 1979 standard run. *Beitr. Phys. Atmosph.*, 61(4), 344-354.

- Kraus, E.B. and J.S. Turner (1967): A one-dimensional model of the seasonal thermocline, Part II. *Tellus*, 19, 98-105.
- Lemke, P. (1987): A coupled one-dimensional sea ice- ocean model. *J. Geophys. Res.*, 92, 13164-13172.
- Lemke, P., W.B. Owens and W.D. Hibler III (1990): A coupled sea ice-mixed layer-pycnocline model for the Weddell Sea. *J. Geophys. Res.*, 95(C6), 9513-9525.
- Leppäranta, M. and W.D. Hibler III (1985): The role of plastic ice interaction in marginal ice zone dynamics. *J. Geophys. Res.*, 90(C11), 11899-11909.
- Louis, J.F. (1979): A parametric model of vertical eddy fluxes in the atmosphere. *Bound. Layer Met.*, 17, 187-202.
- Maykut, G.A. (1982): Large-scale heat exchange and ice production in the central Arctic. *J. Geophys. Res.*, 87(C10), 7971-7984.
- Mesinger, F. and A. Arakawa (1976): Numerical methods used in atmospheric models. WMO-ICSU Jt.Organizing Committee, Geneva, GARP Publ.Series, No.17.
- Niiler, P.P. and E.B. Kraus (1977): One-dimensional models of the upper ocean. In: *Modelling and Prediction of the Upper Layers of the Ocean*, ed: E.B. Kraus, Pergamon Press, New York, 143-172.
- Owens, W.B. and P. Lemke (1990): Sensitivity studies with a sea ice - mixed layer- pycnocline model in the Weddell Sea. *J. Geophys. Res.*, 95(C6), 9527-9538.
- Parkinson, C.L. and W.M. Washington (1979): A large-scale numerical model of sea ice. *J. Geophys. Res.*, 84, 311-337.
- Semtner, A.J. jr. (1976): A model for the thermodynamic growth of sea ice in numerical investigations of climate. *J. Phys. Oceanogr.*, 6, 379-389.
- Stössel, A. (1990): *Meereismodellierung im Südlichen Ozean*. Max-Planck-Institut für Meteorologie, Hamburg, Examensarbeit Nr.6.
- Stössel, A. (1991): Application of an atmospheric boundary-layer model to a large-scale coupled sea-ice-oceanic mixed-layer model for the Southern Ocean. *Ann. Glaciology*, 15, 191-195.

- Stössel, A. (1991): Southern Ocean sea-ice simulations forced with operationally derived atmospheric analyses data. Max-Planck-Institut für Meteorologie, Hamburg, Report No.65.
- Stössel, A. (1992): Sensitivity of Southern Ocean sea-ice simulations to different atmospheric forcing algorithms. Tellus, in press.
- Stössel, A., P. Lemke and W.B. Owens (1990): Coupled sea ice- mixed layer simulations for the Southern Ocean. J. Geophys. Res., 95(C6), 9539-9555.
- Stössel, A. and M. Claussen (1992): A new atmospheric surface-layer scheme for a large-scale sea-ice model. Max-Planck-Institut für Meteorologie, Hamburg, Report No.95.
- Trenberth, K.E. and J.G. Olson (1988): ECMWF global analyses 1979-1986: circulation statistics and data evaluation. NCAR, Boulder, Colorado, Techn.Note, TN-300 + STR.

Acknowledgements:

Thanks are due to P. Lemke for a review of the manual, as well as several users, especially S. Legutke and M. Scheduikat, for the detection of bugs in the model code.

This work was mainly sponsored by SFB 318.

Appendix A MODEL HEADER

```

C=====
C=====SIMOD11=====
C=====
C  Cycles:
C    -The model can alternatively been run for cycles 6, 7, 8 and 11.
C    -The present cycle is indicated in the head line and is deter-
C      mined by the following characteristics:
C      -ABLFIX=0. and SURFWIN=0. and ECMTYP=0. for CYCLE 6.
C      -ABLFIX=0. and SURFWIN=1. and ECMTYP=0. for CYCLE 7.
C      -ABLFIX=1. and SURFWIN=1.           for CYCLE 8.
C      -ABLFIX=0. and SURFWIN=1. and ECMTYP=1. for CYCLE 11.
C=====
C  Updated version:
C    -28.08.92: - 30-day run, cycle 11
C=====
C  Modifications to the first version of 02.08.91:
C    -RWSTAB, RISTAB: correction of ZA
C    -OBUDGET, BUDGET: addition of COMMON/FRWND
C    -ADJUDEX: CL -> CLO
C    -SHWARA: 1353 -> 1367 (acc. to Washington & Parkinson 86, p. 103)
C    -MAIN: loop 132: FW*RHWOAT/RHOICE
C    -INIT: TAUX, TAUY -> loop 280
C    -COMMON/PRESS: -> P(0:L,0:M)
C    -RELCON: in 'coordinate transformation' part -> TMP as edge var.
C    -STAB: FLAG deleted and ZOL/ZLOG: + -> -
C    -GROWTH: -loop 10: TMP=SH -> TMP=RH*A
C              -loop 15: RH=SH-TMP2... -> ...+TMP2...
C              -introduction of snow to ice conversion
C    -PMLEX: loop 50: TMP=...(1.-FLAG))
C=====
C    PROGRAM ICEMODEL(INPUT,OUTPUT,TAPE10,TAPE11,TAPE12,TAPE20,TAPE13,
C      1TAPE15,TAPE16,TAPE17,TAPE18,TAPE19,TAPE8,TAPE14)
C=====
C  Main-code programmed by:
C    William D. Hibler III CRREL, Hanover 1979
C  Reprogrammed and extended by:
C    W.Brechner Owens MPI, Hamburg Aug.87
C    Peter Lemke MPI, Hamburg Aug.87
C  Modified and extended by:
C    Achim Stoessel MPI, Hamburg Jul.92
C  Purpose:
C    -Dynamic-thermodynamic simulation of Sea Ice [SI] optionally
C      coupled to: -Oceanic Mixed Layer model [OML]
C                  -Atmospheric Surface Layer model [ASL]
C                  -Atmospheric Boundary Layer model [ABL]
C  Method:
C    -main program combines various subroutines and controls outputs
C    -coordinates: orthogonal curvilinear (alternatively performable
C      in cartesian or spherical coordinates)

```

```

C     -domain of integration is allowed to be 'open' at lateral edges
C     -cyclic boundary conditions are provided for circumpolar studies
C     -horizontal grid: Arakawa 'B'
C     -time stepping: leapfrog-trapezoidal
C Structure:
C     ICEMODEL==>INIT=====>BCSINIT
C         ==>OUTSM(LOLD)
C         ==>BCSH(LOLD)
C         ==>BCSV(LOLD)
C     ----->==>FORFLD=====>BCSQ
C     |
C     | <--->PRESS(LOLD)
C     |   ==>INITREL=====>OUTBCS
C     |   =====>RELCON(LOLD,LOLD)==>BCOEF(LOLD)
C     |   =====>RELAX(LOLD,LNEW)==>DDX(LNEW)
C     |   =====>DDY(LNEW)
C     |   =====>MADV(LOLD,LNEW)
C     | ->==>PLAST(LOLD)=====>STRAIN(LOLD)
C     |   =====>OUTBCS
C     |   ==>RELCON(LOLD,LOLD)
C     |   ==>RELAX(LOLD,3)
C     |   ==>PLAST(3)
C     |   ==>RELCON(LOLD,3)
C     |   ==>RELAX(3,LNEW)
C     |   ==>SADVECT(LOLD,LNEW)
C     |   ==>BCSH(LNEW)
C     |   ==>SADVECT(LNEW,LNEW)
C     |   ==>SDIFFUS(LOLD)-->BCSFLX
C     |   ==>BCSH(LNEW)
C     |   ==>GROWTH(LOLD,LNEW)==>SHDEF(LNEW)=====>STRAIN(LNEW)
C     |   ==>SHWARA
C     |   ==>OBUDGET/ECMBUDO/EKMAO
C     |   ==>BUDGET/ECMBUDI/EKMAH
C     |   ==>PMLEX
C     |
C     |   ==>OUTSM(LNEW)
C     |   ==>BCSH(LNEW)
C     |   LOLD<-->LNEW---
C     |
C     |-----<-----

```

Interface:

```

C     -INPUT,OUTPUT: standard control output
C     -TAPE10: definition masks for domain
C     -TAPE11: wind forcing
C     -TAPE12: oceanic forcing (temperature, salinity, currents)
C     -TAPE20: ice compactness results for selected dates (plots)
C     -TAPE13: atmospheric temperature forcing
C     -TAPE15: ice velocity results for plots
C     -TAPE16: results printed in domain's shape
C     -TAPE17: various results for plots
C     -TAPE18: accumulated results for summation plots
C     -TAPE19: humidity forcing
C     -TAPE8 : precipitation forcing
C     -TAPE14: atmospheric pressure forcing

```

```

C Externals(subroutines):
C   -INIT:      sets model parameters and initial fields
C   -OUTSM:     smoothes variables in outflow grid cells
C   -BCSH:      sets cyclic boundary cond. for values in grid center
C   -BCSV:      sets cyclic boundary cond. for values at grid edge
C   -FORFLD:    reads in forcing fields
C   -PRESS:     calculates ice strength
C   -INITREL:   performs initial relaxation to balance initial values
C   -PLAST:     calculates viscosities
C   -RELCON:    calculates diagnostic terms of momentum balance
C   -RELAX:     solves momentum balance by overrelaxation
C   -SADVECT:   calculates advection terms for continuity equation
C   -SDIFFUS:   calculates diffusion terms for continuity equation
C   -GROWTH:    represents thermodynamic part of the model
C   -DRUCKF:    prints integer results in domain-mask shape
C References:
C   -Hibler,W.D.,III(1979): A dynamic thermodynamic sea ice model.
C     J.Phys.Oceanogr.,9, 815-846.
C   -Hibler,W.D.(1980): Documentation for a two-level dynamic-thermo-
C     dynamic sea ice model. CRREL, Hanover, N.H., Spec. Rep., 80-8.
C   -Hibler,W.D.(1984): The role of sea ice dynamics in modeling CO2
C     increases. In: Climate processes and climate sensitivity,
C     eds.: J.Hansen and T.Takahashi, Geophys.Monogr.,29,238-253.
C   -Hockney,R.W. and C.R.Jesshope (1981): Parallel computers, archi-
C     tecture, programming and algorithms. Adam Hilger LTD, Bristol.
C   -Koch,C.(1988): A coupled sea ice - atmospheric boundary layer
C     model. Part I: Description of the model and 1979 standard run.
C     Beitr.Phys.Atmosph., 61(4), 344-354.
C   -Lemke,P., W.B.Owens and W.D.Hibler III(1990): A coupled sea ice -
C     mixed layer - pycnocline model for the Weddell Sea. J.Geophys.
C     Res., 95(C6), 9513-9525.
C   -Leppaeranta,M. and W.D.Hibler III (1985): The role of plastic ice
C     interaction in marginal ice zone dynamics. J.Geophys.Res., 90,
C     (C6), 11899-11909.
C   -Louis,J.F.(1979): A parametric model of vertical eddy fluxes in
C     the atmosphere. Bound.Layer Met.,17,187-202.
C   -Mesinger,F. and A.Arakawa (1976): Numerical Methods used in atmo-
C     spheric models. GARP Publ.Ser.No.17.
C   -Owens,W.B. and P.Lemke(1990): Sensitivity Studies with a sea ice-
C     mixed layer - pycnocline model in the Weddell Sea. J.Geophys.
C     Res., 95(C6), 9527-9538.
C   -Stoessel,A.(1991): Southern Ocean sea-ice simulations forced with
C     operationally derived atmospheric analysis data. Max-Planck-
C     Inst. f. Meteorologie, Hamburg, Report No. 65.
C   -Stoessel,A., P.Lemke and W.B.Owens(1990): Coupled sea ice - mixed
C     layer simulations for the Southern Ocean. J.Geophys.Res., 95
C     (C6), 9539-9555.
C   -Stoessel,A.(1990): Meereismodellierung im Suedlichen Ocean. Max-
C     Planck-Inst.f.Meteorologie, Hamburg, Examensarbeit Nr.6.
C=====
C     PARAMETER(L=74, M=14, LM=L-1, MM=M-1, LP=L+1, MP=M+1, LDO=4*L)
C=====

```

```

C Parameter:
C   -L: number of grid points in X-direction (even number only!)
C   -M: number of grid points in Y-direction (even number only!)
C=====
COMMON/CORR/FM(0:M),F(M),COSPHI(0:M),SINPHI(0:M)
C=====
C Common CORR: contains coriolis parameter related variables
C   -FM:      Coriolis parameter for grid center [1/s]
C   -F:       Coriolis parameter for grid edge [1/s]
C   -COSPHI:  COS of grid center latitude []
C   -SINPHI:  SIN of grid center latitude []
C=====
COMMON/IPARM/RHOICE,H0,HNU,HNU2,ARMIN,ARMAX,HMIN,RHOSNO,CC
C=====
C Common IPARM: contains sea ice related parameters
C   -RHOICE:  sea ice density [kg/m**3]
C   -H0:      lead closing parameter for ice compactness equation [m]
C   -HNU:     harmonic diffusion coefficient [m**2/s]
C   -HNU2:    biharmonic diffusion coefficient [m**4/s]
C   -ARMIN:   minimum (cut off) ice compactness [100%=1]
C   -ARMAX:   maximum ice compactness [100%=1]
C   -HMIN:    minimum (cut off) ice thickness [m]
C   -RHOSNO:  snow density [kg/m**3]
C   -CC:      volumetric heat capacity of water [J/m**3/K]
C=====
COMMON/DRV/DX,DXSQ,DY,DYSQ,SX2,SY2,SXY
C=====
C Common DRV: contains grid size related parameters
C   -DX:      grid size in X-direction (before use of metric!)[m]
C   -DXSQ:    DX*DX [m**2]
C   -DY:      grid size in Y-direction [m]
C   -DYSQ:    DY*DY [m**2]
C   -SX2:     0.5/DXSQ [1/m**2]
C   -SY2:     0.5/DYSQ [1/m**2]
C   -SXY:     0.25/(DX*DY) [1/m**2]
C=====
COMMON/STP/T,DT,NTMES,NRST,NRREC,NPLT,NSTAT,IIC,NFLD,NSTA
C=====
C Common STP: contains time step related parameters
C   -T:       current time step [s]
C   -DT:      time step []
C   -NTMES:   number of time steps for specific integration []
C   -NRST:    time steps between writing RESTART record []
C   -NRREC:   number of RESTART records to read []
C   -NPLT:    time steps between plot outputs []
C   -NSTAT:   time steps between statistics output []
C   -IIC:     running time step (INTEGER)[]
C   -NFLD:    time step limit for beginning of output []
C   -NSTA:    time steps between areal prints (NSTAT + 5)[]
C=====
COMMON/COORD/PM(0:L,0:M),PN(0:L,0:M),DNDX(L,M),DMDY(L,M)
C=====

```

```

C Common COORD: contains metric coefficients
C   -PM:      metric coefficients for X-direction []
C   -PN:      metric coefficients for Y-direction []
C   -DNDX:    metric term for centripetal forces in Y-direction []
C   -DMDX:    metric term for centripetal forces in X-direction []
C=====
COMMON/VEL/U(L,M,3),V(L,M,3)
C=====
C Common VEL: ice velocity field (defined st grid edge points)
C   -U:      X-component of ice velocity [m/s]
C   -V:      Y-component of ice velocity [m/s]
C=====
COMMON/THCK/H(0:L,0:M,2),A(0:L,0:M,2),HSN(0:L,0:M,2)
C=====
C Common THCK: thickness fields (defined on grid center points)
C   -H:      mean ice thickness [m]
C   -A:      ice compactness [100%=1]
C   -HSN:    snow thickness [m]
C=====
COMMON/FRWND/RHOAIR,CDWIN,SINWIN,COSWIN,UWIN(L,M),VWIN(L,M)
C=====
C Common FRWND: atmospheric parameters and wind forcing
C   -RHOAIR: air density [kg/m**3]
C   -CDWIN:  atmospheric drag coefficient []
C   -SINWIN: SIN of ABL turning angle []
C   -COSWIN: COS of ABL turning angle []
C   -UWIN:   X-component of wind velocity [m/s]
C   -VWIN:   Y-component of wind velocity [m/s]
C=====
COMMON/FRWAT/RHOWAT,CDWAT,SINWAT,COSWAT,UWAT(L,M),VWAT(L,M)
C=====
C Common FRWAT: oceanic parameters and current forcing
C   -RHOWAT: water density [kg/m**3]
C   -CDWAT:  oceanic drag coefficient []
C   -SINWAT: SIN of OBL turning angle []
C   -COSWAT: COS of OBL turning angle []
C   -UWAT:   X-component of current velocity [m/s]
C   -VWAT:   Y-component of current velocity [m/s]
C=====
COMMON/THFOR/TAIR(0:L,0:M),TD(0:L,0:M),ACL(0:M),PA(0:L,0:M)
1,UG(0:L,0:M),TA(0:L,0:M),RPREC(0:L,0:M)
C=====
C Common THFOR: atmospheric thermodynamic forcing variables
C   -TAIR:   air temperature [C]
C   -TD:     relative humidity [%]
C   -ACL:    cloudiness [100%=1]
C   -PA:     surface air pressure [hPa -> Pa]
C   -UG:     wind velocity [m/s]
C   -TA:     air temperature [K]
C   -RPREC:  precipitation rate [mm/month -> m/s]
C=====
COMMON/THPAR/SUBL,VAPL,D3,CON,ALBI,ALBM,ALBW,ALBSN,ALBSNM,TMELT,

```

1TFREZ, CONSN

```

C=====
C Common THPAR: contains various thermodynamic parameters
C   -SUBL:    latent heat of sublimation [J/kg]
C   -VAPL:    latent heat of vaporization [J/kg]
C   -D3:      Stefan-Boltzmann constant * emissivity [W/m**2/K**4]
C   -CON:     thermal conductivity of sea ice [W/m/K]
C   -ALBI:    sea ice albedo []
C   -ALBM:    melting sea ice albedo []
C   -ALBW:    open water albedo []
C   -ALBSN:   snow albedo []
C   -ALBSNM:  melting snow albedo []
C   -TMELT:   melting point [K]
C   -TFREZ:   freezing point for ocean [C]
C   -CONSN:   thermal conductivity of snow [W/m/K]
C=====
COMMON/VISCP/PSTAR,CSTAR,ECCEN,ZMAX,ZMIN,GMIN,ECM2
C=====
C Common VISCP: contains viscosity parameters
C   -PSTAR:   empirical ice strength parameter [N/m**2]
C   -CSTAR:   empirical ice strength constant []
C   -ECCEN:   ratio of compressive to shear strength []
C   -ZMAX:    limiting factor for maximum bulk viscosity []
C   -ZMIN:    minimum bulk viscosity [kg/s]
C   -GMIN:    maximum viscous creep rate [1/s]
C   -ECM2:    1/ECCEN**2
C=====
COMMON/PRESS/P(L,M)
C=====
C Common PRESS: equation of state for ice pressure
C   -P:       ice strength [N/m]
C=====
COMMON/TEMP/TICE(0:L,0:M)
C=====
C Common TEMP: surface temperature
C   -TICE:    surface temperature of ice or snow, resp.[C]
C=====
COMMON/TEMPM/TICM(0:L,0:M,7)
C=====
C Common TEMPM: surface temperatures for seven-level heat balance
C   -TICM:    surface temp. for seven ice thickness categories [C]
C=====
COMMON/RELAXP/MMAX,VRMAX,WT
C=====
C Common RELAXP: parameters for overrelaxation routine
C   -MMAX:    maximum iteration steps []
C   -VRMAX:   cut off velocity difference between iteration steps[m/s]
C   -WT:      relaxation factor []
C=====
COMMON/MASK/VM(L,M),HM(0:L,0:M),OM(0:L,0:M),FLM(0:L,0:M,2)
C=====
C Common MASK: contains definition points for specific domain

```

```

C   -VM:      mask for grid edge points []
C   -HM:      mask for grid center points []
C   -OM:      mask to separate outflow grid points []
C   -FLM:     mask for fluxes normal to boundaries []
C=====
COMMON/PML/QS(0:L,0:M),QT(0:L,0:M),QH(0:L,0:M),QSB(0:L,0:M),
1QTB(0:L,0:M),QHB(0:L,0:M),QDS(0:L,0:M),QDT(0:L,0:M),
2QHSTO(0:L,0:M),HS(0:L,0:M),HT(0:L,0:M),QV(0:L,0:M),QRHO(0:L,0:M),
3QW(0:L,0:M),IEN(0:L,0:M),FW(0:L,0:M),MLFIX
C=====
C   Common PML: contains variables for OML model
C   -QS:      OML salinity [ppt]
C   -QT:      OML temperature [C]
C   -QH:      OML depth [m]
C   -QSB:     salinity at base of second oceanic layer [ppt]
C   -QTB:     temperature at base of second oceanic layer [C]
C   -QHB:     depth of second oceanic layer [m]
C   -QDS:     halocline thickness [m]
C   -QDT:     thermocline thickness [m]
C   -QHSTO:   heat storage in equivalent [m] of ice thickness
C   -HS:      salinity content of water column [ppt*m]
C   -HT:      heat content of water column [C*m]
C   -QV:      cubic ice vel. for OML kinetic energy input [(m/s)**3]
C   -QRHO:    surface buoyancy flux [1/s]
C   -QW:      kinetic energy input for OML [(m/s)**3]
C   -IEN:     flag for calculation of entrainment []
C   -FW:      net freezing rate [m]
C   -MLFIX:   flag for either fixed or variable OML []
C=====
COMMON/GEO/PI,RAD,SOL,COSZ(0:M)
C=====
C   Common GEO: parameters for solar radiation
C   -PI:      circle number []
C   -RAD:     factor for conversion of degree into radiant (PI/180)[]
C   -SOL:     solar constant times factor for sun distance [W/m**2]
C   -COSZ:    cosine of zenith distance of the sun []
C=====
COMMON/ABLM/ZOW(0:L,0:M),ZOI,CLB,CLO,FAKTH,ABLFIX,SURFWIN,ECMTYP
C=====
C   Common ABLM: parameters for ABL model
C   -ZOW:     roughness length over water [m]
C   -ZOI:     roughness length over ice [m]
C   -CLB:     rhoice * lat. heat of fusion at ice bottom [J/m**3]
C   -CLO:     rhoice * lat. heat of fusion at ice surface [J/m**3]
C   -FAKTH:   rhoair * v.Karman const.* spec.heat of dry air[J/m**3/K]
C   -ABLFIX:  switch for simulation with or without ABL []
C   -SURFWIN: switch for fixed wind turning or calculated by ABL model
C   -ECMTYP:  switch for simulation with ASL or ABL
C=====
COMMON/TAU/CD(0:L,0:M),SINBET(0:L,0:M),COSBET(0:L,0:M),
1BETA(0:L,0:M),TAUX(L,M),TAUY(L,M)
C=====

```

```

C Common TAU: variables of ABL model derived dynamic forcing of sea ice
C   -CD:      drag coefficient []
C   -SINBET:  SIN of wind turning angle []
C   -COSBET:  COS of wind turning angle []
C   -BETA:    wind turning angle [deg]
C   -TAUX:    X-component of wind stress [N/m**2]
C   -TAUY:    Y-component of wind stress [N/m**2]
C=====
COMMON/FLUX/FLSE(0:L,0:M),FLLA(0:L,0:M),WMUE1(0:L,0:M)
1,UST1(0:L,0:M),TMPL1(0:L,0:M)
C=====
C Common FLUX: heat flux and ABL stability related variables
C   -FLSE:    sensible heat flux [W/m**2]
C   -FLLA:    latent heat flux [W/m**2]
C   -WMUE1:   stability parameter []
C   -UST1:    friction velocity [m/s]
C   -TMPL1:   Richardson number or mod.Monin-Obukhov length [ ]or[1/m]
C=====
COMMON/OUTFLOW/NOOUT, IOOUT(LDO), JOOUT(LDO)
C=====
C Common OUTFLOW: contains outflow cells
C   -NOOUT:   number of outflow cells []
C   -IOOUT:   X-coordinate of outflow cell []
C   -JOOUT:   Y-coordinate of outflow cell []
C=====
COMMON/PMLPARM/SICE, QHW, QHS, DCVM, ENTMAX, WUP, CW, COSGAM, BETAS, BETAT,
1EPSAA, RTC, STC, QTOC
C=====
C Common PMLPARM: contains parameters for OML model
C   -SICE:    sea ice salinity [ppt]
C   -QHW:     emp. parameter for dissipation of mechanical energy [m]
C   -QHS:     emp. parameter for dissipation of convective energy [m]
C   -DCVM:    upper limit for dissipation of convective energy []
C   -ENTMAX:  upper limit for entrainment velocity [m]
C   -WUP:     upwelling velocity (specified empirically) [m/s]
C   -CW:      drag coefficient for kinetic energy input []
C   -COSGAM:  COS of current turning angle []
C   -BETAS:   expansion coefficient for salinity [1/ppt]
C   -BETAT:   expansion coefficient for temperature [1/K]
C   -EPSAA:   limitations for entrainment velocity and conv. [(m/s)**2]
C   -RTC:     time constant for mixed layer retreat []
C   -STC:     salinity time constant []
C   -QTOC:    oceanic heat flux (specified) [W/m**2]
C=====
COMMON/SNOFLG/SNOFLG
C=====
C Common SNOFLG: contains switch for inclusion of snow
C=====

```


Appendix B CRAY BATCHJOB TO RUN THE MODEL

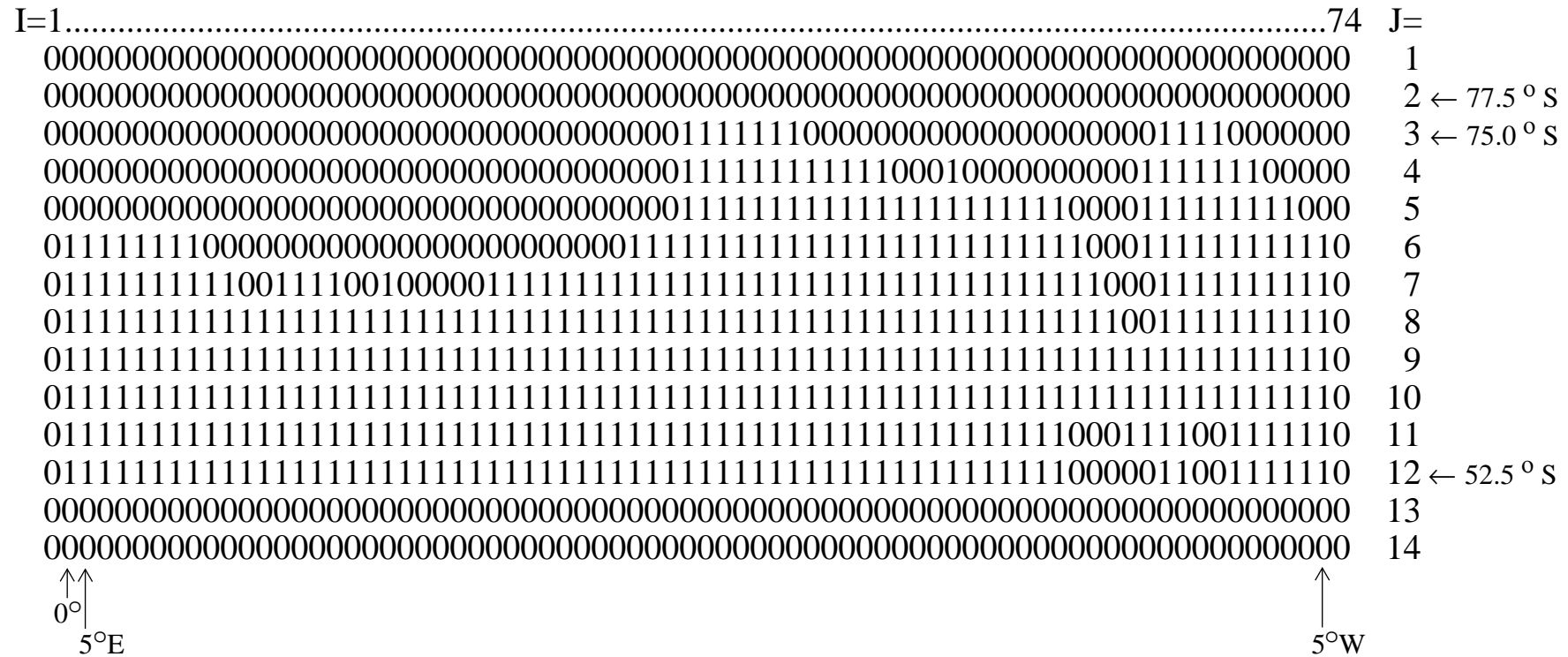
```

# QSUB-q S3
# QSUB-r seaice
# QSUB-eo
# QSUB-x
set -x
set -e
date
PERM=/pool/POST/seaice
OUTDIR=/mf/b/k204002
TMP=$TMPDIR
cd $TMP
cp $PERM/SIMOD prog.f
cft77 -dp -exm prog.f
segldr -o prog.x prog.o
env FILENV=assgn-1 assign -a $PERM/mask u:10
env FILENV=assgn-1 assign -a $PERM/tsuvwg u:12
env FILENV=assgn-1 assign -a $PERM/prj u:8
env FILENV=assgn-1 assign -a $PERM/uve u:11
env FILENV=assgn-1 assign -a $PERM/tae u:13
env FILENV=assgn-1 assign -a $PERM/rhe u:19
env FILENV=assgn-1 assign -a $PERM/pae u:14
env FILENV=assgn-1 assign -a res16 u:16
env FILENV=assgn-1 assign -a res18 u:18
env FILENV=assgn-1 assign -a res15 u:15
env FILENV=assgn-1 assign -a res17 u:17
env FILENV=assgn-1 assign -a res20 u:20
ja -t
ja -m prog.ja
env FILENV=assgn-1 prog.x > control.out 2> err.out
ja -cfsld prog.ja > jacc.out
ja -t
#
# copy output
#
cp res16 $OUTDIR/SISTA
cp res18 $OUTDIR/SISUM
cp res20 $OUTDIR/SINIM
cp res15 $OUTDIR/SIUV
cp res17 $OUTDIR/SIISO
cat err.out >> control.out
cat jacc.out >> control.out
cp control.out $OUTDIR/seaice.cntl
#
ls -l
exit

```

This example job can be found in the global accessible file /pool/POST/seaice.job on the CRAY-2S.

Appendix D LAND-SEA MASKS



PAGE 59

DKRZ Sea-Ice Model Documentation

Figure 1 : Southern ocean mask (50° S - 80° S, circumpolar) for vector variables VM(L,M) with L=74, M=14. Zonal spacing is 5°, while meridional spacing is 2.5°. Note that the first and last actual gridpoint in zonal direction (near the seam at λ=0°) are I=2 and I=73. In meridional direction VM starts with J=3 and ends with J=12.

